

Ancillary Steric Effects on the Activation of SiH Bonds in Arylsilazido Rare-Earth Compounds

Kasuni C. Boteju, Amrit Venkatesh, Yang-Yun Chu, Suchen Wan, Arkady Ellern, Aaron J. Rossini, and Aaron D. Sadow*

Cite This: *Organometallics* 2021, 40, 1654–1669

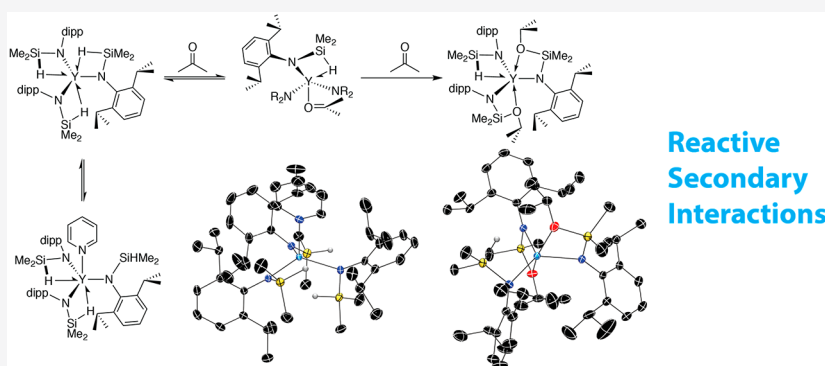
Read Online

ACCESS |

Metrics & More

Article Recommendations

Supporting Information



ABSTRACT: Three new hydrosilazido ligands, $-N(\text{SiHMe}_2)\text{Aryl}$ (Aryl = Ph, 2,6- $\text{C}_6\text{Me}_2\text{H}_3$ (dmp), 2,6- $\text{C}_6\text{iPr}_2\text{H}_3$ (dipp)) and their rare-earth complexes $\text{Ln}\{\text{N}(\text{SiHMe}_2)\text{Aryl}\}_3(\text{THF})_n$ (Ln = Sc, Y, Lu; Aryl = Ph, $n = 2$; Aryl = dmp, $n = 1$; Aryl = dipp, $n = 0$) were synthesized to study the relationships among ligand steric properties, secondary Ln \leftarrow H–Si bonding, and the reactivity of amide and SiH groups. In these compounds, the steric encumbrance of the aryl group was systematically increased from phenyl to 2,6-dimethylphenyl to 2,6-diisopropylphenyl. NMR, IR, and X-ray diffraction studies of the complexes characterize the number of secondary interactions and additional THF ligands coordinated to the rare-earth centers. The complexes with the smallest phenylsilazido ligands, $\text{Ln}\{\text{N}(\text{SiHMe}_2)\text{Ph}\}_3(\text{THF})_2$, contain features associated with three nonbridging 2-center-2-electron (2c-2e) Si–H bonds. Characterization of intermediate-sized $\text{Ln}\{\text{N}(\text{SiHMe}_2)\text{dmp}\}_3\text{THF}$ reveals three and two Ln \leftarrow H–Si interactions for yttrium and lutetium analogues, respectively, with both metals having one coordinated THF per complex. $\text{Ln}\{\text{N}(\text{SiHMe}_2)\text{dipp}\}_3$ is formed solvent-free, and all three ligands adopt Ln \leftarrow H–Si bonding modes. The reaction between $\text{Ln}\{\text{N}(\text{SiHMe}_2)\text{dipp}\}_3$ and ketones provides the hydrosilylated product via addition of C=O and Si–H bonds, which occurs rapidly even at low temperature. This reaction is proposed to occur through an associative mechanism on the basis of negative activation entropy measured for substitution of pyridine in $\text{Ln}\{\text{N}(\text{SiHMe}_2)\text{dipp}\}_3\cdot\text{NC}_5\text{H}_5$.

INTRODUCTION

Low-coordinate and low-electron-count homoleptic rare-earth compounds of the type LnX_3 often require bulky ligands, whose coordination properties also include labile secondary interactions, to stabilize the metal center.¹ These two features can be included in the rational design of new electrophilic pseudo-organometallic compounds that have a range of uses in synthesis^{2–6} and catalysis,^{7–10} as well as potential applications derived from their unique electronic and magnetic properties.^{11,12} However, neither the relative contributions of secondary interactions and steric properties of the ligands for stabilization of solvent-free and salt-free highly electrophilic organometallic and pseudo-organometallic compounds nor the effect of these interactions on reactivity has been systematically explored.

A few disilazido ligands have been used to support trivalent rare-earth-metal centers with low coordination geometries, including hexamethyldisilazide $\text{N}(\text{SiMe}_3)_2$,^{13–17} the smaller tetramethyldisilazide $\text{N}(\text{SiHMe}_2)_2$,¹⁸ pentamethyl-*tert*-butyldisilazide $\text{N}(\text{SiMe}_3)(\text{SiMe}_2\text{tBu})$, and the bulkiest tetramethyldi-*tert*-butyldisilazide $\text{N}(\text{SiMe}_2\text{tBu})_2$.¹⁹ The $\text{N}(\text{SiMe}_2)_2$ ligand and its rare-earth compounds have been used extensively as starting materials, catalysts, and reactants for grafting onto surfaces.^{1,15,20} These species have interesting structural features,

Received: March 16, 2021

Published: June 2, 2021



including trigonal-pyramidal geometries, even though the metal centers are typically f^0 and contain secondary $\text{Ln} \leftarrow \text{C}-\text{Si}$ interactions.^{1,21–25} $\text{Ln}\{\text{CH}(\text{SiMe}_3)_2\}_3$ compounds also reveal secondary $\text{Ln} \leftarrow \text{C}-\text{Si}$ interactions ($\text{Ln} = \text{La}, \text{Ce}, \text{Y}, \text{Lu}$).^{26–29} In contrast, ligands with greater steric hindrance give trigonal-planar structures, while the smallest ligand, $\text{N}(\text{SiHMe}_2)_2$, typically provides solvent-coordinated compounds or N-bridged dimeric species.^{30,31} For example, the compounds $\text{Ln}\{\text{N}(\text{SiHMe}_2)_2\}_3(\text{THF})_n$ ($\text{Ln} = \text{Sc}, n = 1; \text{Y}, n = 1, 2; \text{Lu}, n = 2; \text{La}, n = 2$) are prepared by salt metathesis reactions of $\text{LiN}(\text{SiHMe}_2)_2$ and $\text{LnCl}_3(\text{THF})_x$.³⁰ Alternatively, the acidic $\text{HN}(\text{SiHMe}_2)_2$ ($\text{p}K_a = 22.8$ in benzene/THF)³² reacts with $\text{La}\{\text{N}(\text{SiMe}_3)_2\}_3$ to give THF-free, dimeric $[\text{La}\{\text{N}(\text{SiHMe}_2)_2\}_2]_2$.³¹ These compounds form bridging $\text{M} \leftarrow \text{H}-\text{Si}$ secondary interactions that increase the electron count and ligand bond number as L-type donors in these otherwise coordinatively unsaturated species.^{33,34} The ^1H NMR spectroscopic features (chemical shift, one-bond silicon–hydrogen coupling constants) and IR stretching frequencies of the SiH group are distinct from those of other functional groups (e.g., CH, SiMe_3), which facilitates characterization and studies of the compounds' reactivity. These features are also responsive to the presence and possibly the strength of $\text{Ln} \leftarrow \text{H}-\text{Si}$ interactions.

The silazido ligand $\text{N}(\text{SiHMe}_2)t\text{Bu}$ also supports homoleptic compounds $\text{Ln}\{\text{N}(\text{SiHMe}_2)t\text{Bu}\}_3$ ($\text{Ln} = \text{Sc}, \text{Y}, \text{Er}, \text{Lu}$).^{35,36} Bonding of these rare-earth silazidos includes three secondary $\text{Ln} \leftarrow \text{H}-\text{Si}$ interactions (one for each ligand), which are assigned by low $^1J_{\text{Si}-\text{H}}$ values in ^1H NMR spectra, by low frequency ν_{SiH} ($<2000 \text{ cm}^{-1}$) in the IR spectra, and from single-crystal X-ray diffraction studies. The structures are slightly distorted from trigonal planar to pyramidal, as defined by the sum of the angles around the metal center ($\sum_{\text{N}_\text{LnN}} < 360^\circ$; Sc, 348.6° ; Lu, 349.0° ; Y, 351.3°). In addition, a set of solvent-coordinated rare-earth compounds of the same ligand has been reported: $\text{Ln}\{\text{N}(\text{SiHMe}_2)t\text{Bu}\}_3\text{L}$ ($\text{Ln} = \text{Y}, \text{Lu}$; $\text{L} = \text{THF}, \text{Et}_2\text{O}$). The values of $^1J_{\text{Si}-\text{H}}$ and ν_{SiH} of $\text{Ln}\{\text{N}(\text{SiHMe}_2)t\text{Bu}\}_3\text{THF}$ ($\text{Ln} = \text{Y}, \text{Lu}$) are higher than those of solvent-free compounds. Yet, all three SiH form $\text{Ln} \leftarrow \text{H}-\text{Si}$ interactions in the solid-state structures of $\text{Ln}\{\text{N}(\text{SiHMe}_2)t\text{Bu}\}_3\text{THF}$.

Commonly, the amide and alkyl ligands in homoleptic compounds behave as bases in reactions with weakly acidic organic species, such as enolizable ketones, and are substituted by other X-type ligands through protonolysis reactions. The permethylated disilazido ligand is also relatively acidic ($\text{HN}(\text{SiMe}_3)_2$ $\text{p}K_a = 25.8$), although not as acidic as $\text{HN}(\text{SiHMe}_2)_2$.³² The acidity of disilazanes creates a thermodynamic limitation on protonolytic substitutions of rare-earth disilazidos, which are needed for the synthesis of new catalysts.

A second reactivity pattern is associated with alkyl ligands containing secondary β -agostic-type CH interactions, namely β -hydrogen elimination or its microscopic reverse, insertion into a $\text{M}-\text{H}$ bond.³⁷ No such relationship is established between $\text{Ln} \leftarrow \text{E}-\text{Si}$ ($\text{E} = \text{H}, \text{C}$) and their reactivity patterns.³⁸ Instead, $\text{Ln} \leftarrow \text{E}-\text{Si}$ interactions typically are structural features of electron-poor complexes.^{32,39} Recently, a few examples reveal that $d^0 \text{M} \leftarrow \text{H}-\text{Si}$ or $\text{Ln} \leftarrow \text{H}-\text{Si}$ interactions are reactive. The cationic or zwitterionic zirconium disilazidos $[\text{Cp}_2\text{ZrN}(\text{SiHMe}_2)_2]^+$ and $\text{Cp}_2\text{Zr}\{\text{N}(\text{SiHMe}_2)(\text{SiHMeCH}_2\text{B}(\text{C}_6\text{F}_5)_3)\}$ react with acetone and formaldehyde to give hydrosilylation products $[\text{Cp}_2\text{ZrN}(\text{SiMe}_2\text{OR})_2]^+$ ($\text{R} = \text{Me}, \text{CHMe}_2$) or $\text{Cp}_2\text{Zr}\{\text{N}(\text{SiMe}_2\text{OR})(\text{Si}(\text{OR})\text{MeCH}_2\text{B}(\text{C}_6\text{F}_5)_3)\}$.^{40,41}

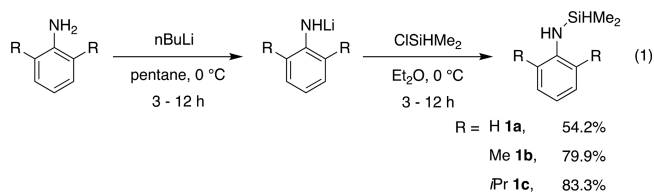
In addition, $[\text{Cp}_2\text{ZrN}(\text{SiHMe}_2)_2]^+$ and 4-dimethylaminopyridine (dmap) react to give a zirconium hydride containing a dmap-coordinated silazido, $[\text{Cp}_2\text{ZrH}\{\text{N}(\text{SiHMe}_2)(\text{SiMe}_2\text{dmap})\}]^+$, suggesting that the silicon is the most accessible electrophilic site in $[\text{Cp}_2\text{ZrN}(\text{SiHMe}_2)_2]^+$. In the initial communication of the present work, we reported that $\text{Y}\{\text{N}(\text{SiHMe}_2)\text{dipp}\}_3$ ($\text{dipp} = 2,6$ -diisopropylphenyl) and acetophenone react via hydrosilylation.⁴² Recently, $\text{La}\{\text{N}(\text{SiHMe}_2)_2\}_3(\text{THF})_2$ was shown to catalyze the hydrosilylation of benzophenone, proposed to occur through addition of the ketone to the silazido SiH, with the turnover-limiting step being protonolytic substitution of $\text{La}-\text{N}(\text{SiMe}_2\text{OCHPh}_2)$.⁴³ The smaller yttrium derivative is not a catalyst for this reaction under related conditions. Moreover, a relationship between the reactivity of the $\text{Ln} \leftarrow \text{H}-\text{Si}$ motif and the spectroscopic and structural features of the compounds is also not yet generally established.

A larger number of silazido ligands of the type $\text{N}(\text{SiMe}_3)\text{-Aryl}$ ($\text{Aryl} = \text{Ph}, 2,6\text{-C}_6\text{Et}_2\text{H}_3, 2\text{-C}_6\text{H}_4\text{Oph}$, and dipp) suggest that the rich, yet underexplored, chemistry comes from a variation of these ligands' steric and electronic features. The bulky ligand containing the o -diisopropylaryl moiety can support the two-coordinate iron compound $\text{Fe}\{\text{N}(\text{SiMe}_3)\text{-dipp}\}_2$.^{44,45} The reaction of $\text{La}(\text{BH}_4)_3(\text{THF})_3$ and $\text{KN}(\text{SiMe}_3)\text{dipp}$ provides the THF-free homoleptic complex $\text{La}\{\text{N}(\text{SiMe}_3)\text{dipp}\}_3$,⁴⁶ whereas reactions of $\text{LiN}(\text{SiMe}_3)\text{dipp}$ and LnCl_3 afford partial substitution.⁴⁷ Rare-earth compounds such as $\text{Ln}\{\text{N}(\text{SiMe}_3)\text{C}_6\text{H}_5\}_3\text{THF}$ ($\text{Ln} = \text{Y}, \text{Lu}$), $[\text{Y}\{\text{N}(\text{SiMe}_3)(2,6\text{-C}_6\text{H}_3\text{Et}_2)\}_3\text{Cl}][\text{Li}(\text{THF})_4]$, and $\text{Lu}\{\text{N}(\text{SiMe}_3)\text{-dipp}\}_2\text{Cl}(\text{THF})$ typically are solvent-coordinated or form "ate" compounds.^{47,48} Donor groups included in the silazido ligand, such as in $\text{Y}\{\text{N}(\text{SiMe}_3)(2\text{-C}_6\text{H}_4\text{Oph})\}_3$, coordinate to the exclusion of THF and LiCl .⁴⁹

In this paper, we have designed a new set of silazido ligands which contain a SiHMe_2 moiety, placing a SiH β with respect to the rare-earth-metal center, and a small, medium, or large aryl group. The steric properties of the aryl group were varied by changing the substituents at the ortho positions, giving $\text{-N}(\text{SiHMe}_2)\text{Aryl}$ ($\text{Aryl} = \text{Ph}, 2,6\text{-C}_6\text{Me}_2\text{H}_3$ (dmp), dipp). A series of rare-earth ($\text{Ln} = \text{Sc}, \text{Y}, \text{Lu}$) compounds containing these silazido ligands have been synthesized to study the influence of the aryl group substituents on the coordination number, geometry, and reactivity of the rare-earth complexes.

RESULTS AND DISCUSSION

Synthesis of Dimethylsilyl Anilides. The deprotonation of aniline derivatives H_2NAryl ($\text{Aryl} = \text{Ph}, \text{dmp}, \text{dipp}$) with $n\text{BuLi}$, followed by the addition of ClSiHMe_2 , provides $\text{HN}(\text{SiHMe}_2)\text{Aryl}$ (eq 1), on the basis of a modification of



the procedures for the preparation of $\text{HN}(\text{SiMe}_3)\text{dipp}$.⁵⁰ A mixture of $\text{HN}(\text{SiHMe}_2)\text{Ph}$ (**1a**) and the disilylaniline $\text{N}(\text{SiHMe}_2)_2\text{Ph}$ was obtained in a 10.5:1 ratio in the reaction of the parent aniline. Further separation of this mixture is not necessary because its reaction with $n\text{BuLi}$ provides pure $\text{LiN}(\text{SiHMe}_2)\text{Ph}$ in the subsequent step (see below). Pure

Table 1. NMR and IR Spectroscopic Data of Silazanes and Silazido Compounds

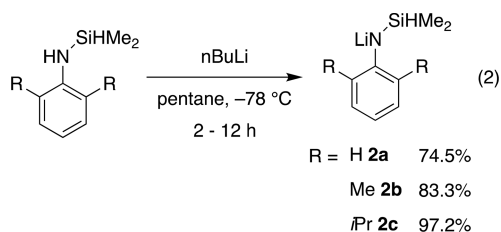
compound	^{29}Si δ_{Si} (ppm)	^1H δ_{SiH} (ppm)	$^1\text{J}_{\text{SiH}}$ (Hz)	^{15}N δ_{N} (ppm)	IR (cm^{-1})
HN(SiHMe ₂)Ph (1a)	-14.2	4.82	200.1	-320.8	2129
HN(SiHMe ₂)dmp (1b)	-10.4	4.87	201.5	-333.5	2126
HN(SiHMe ₂)dipp (1c) ^a	-9.9	4.89	199.2	-343.6	2112
LiN(SiHMe ₂)Ph (2a)	-29.2	4.72	176.9	-280.8	2069
LiN(SiHMe ₂)dmp (2b)	-21.3	5.10	164.8	-305.4	2122, 2056, 1981
LiN(SiHMe ₂)Dipp (2c) ^a	-20.2	5.09	177	n.d. ^b	2022
Sc{N(SiHMe ₂)Ph} ₃ (THF) ₂ (3a)	-21.9	5.24	175.9	-214.1	2113, 2064
Y{N(SiHMe ₂)Ph} ₃ (THF) ₂ (4a)	-24.7	4.95	173.2	-235.0	2117, 2075
Lu{N(SiHMe ₂)Ph} ₃ (THF) ₂ (5a)	-23.0	4.90	173.6	-233.6	2123, 2081
Y{N(SiHMe ₂)dmp} ₃ THF (4b)	-25.3	5.20	151.3	-234.6	2057, 1966
Lu{N(SiHMe ₂)dmp} ₃ THF (5b)	-23.7	5.20	155.8	-235.2	2071, 1902
Sc{N(SiHMe ₂)dipp} ₃ (3c) ^a	-28.1	5.43	142.6	-221.0	2105, 2046
Y{N(SiHMe ₂)dipp} ₃ (4c) ^a	-28.2	5.17	129.2	-239.6	1934, 1883
Lu{N(SiHMe ₂)dipp} ₃ (5c) ^a	-27.6	5.43	127.6	-241.6	1942, 1877
Y{N(SiHMe ₂)dipp} ₃ .NC ₅ H ₅ (4c .py)	-26.5	5.33	150	n.d. ^b	2103, 1959

^aReference 42. ^bn.d. denotes not detected.

HN(SiHMe₂)dmp (**1b**) and HN(SiHMe₂)dipp (**1c**) were obtained after distillation without any issue. Throughout this paper, compounds of N(SiHMe₂)Aryl are labeled on the basis of the substitution of the aryl group by **#a** for phenyl, **#b** for 2,6-dimethylphenyl, and **#c** for 2,6-diisopropylphenyl dimethylsilazido.

Because the NMR (chemical shift and $^1\text{J}_{\text{SiH}}$) and IR (SiH stretching frequency, ν_{SiH}) spectroscopic features of the SiH group are important for characterizing the bridging M–H–Si bonding described below, these data for the (nonbridging) silazane starting materials are given here (Table 1). The ^1H NMR signals for **1a** at 4.82 ppm ($^1\text{J}_{\text{SiH}} = 200.1$ Hz), **1b** at 4.87 ppm ($^1\text{J}_{\text{SiH}} = 201.5$ Hz), and **1c** at 4.89 ppm ($^1\text{J}_{\text{SiH}} = 199.2$ Hz) were assigned to the SiH groups on the basis of the chemical shift and coupling constant values of silazanes. These coupling constants were slightly larger than those for other SiH-substituted silazanes, such as HN(SiHMe₂)tBu ($^1\text{J}_{\text{SiH}} = 192$ Hz),⁵¹ and the disilazane HN(SiHMe₂)₂ ($^1\text{J}_{\text{SiH}} = 170$ Hz).³⁰ The anilines **1a–c** contained bands in their IR spectra at 2129, 2126, and 2112 cm^{-1} , respectively, assigned to the ν_{SiH} mode for each compound. These values are similar to those reported for the IR spectra of HN(SiHMe₂)tBu (2135 and 2104 cm^{-1}) and HN(SiHMe₂)₂ (2120 cm^{-1}).^{30,36}

Deprotonation of **1a–c** with $n\text{BuLi}$ gives the desired lithium silazido species LiN(SiHMe₂)Aryl (**2a–c**; eq 2) in good yields. Compound **2a** is purified by washing the solid product with pentane, while **2b** and **2c** are recrystallized from pentane to obtain analytically pure products.

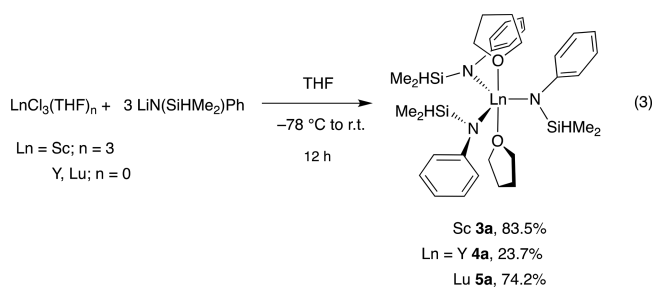


The ^1H NMR spectra of **2a–c** revealed resonances at 4.72 ppm ($^1\text{J}_{\text{SiH}} = 177$ Hz), 5.10 ppm ($^1\text{J}_{\text{SiH}} = 165$ Hz), and 5.09 ppm ($^1\text{J}_{\text{SiH}} = 177$ Hz) ppm, respectively. Note that the signal in the phenylsilazido **2a** appeared at lower frequency in comparison to its silazane precursor, whereas the chemical

shifts for **2b,c** were higher than the corresponding silazanes. The higher NMR frequency for the SiH in LiN(SiHMe₂)R vs HN(SiHMe₂)R is atypical. For example, the SiH signals in ^1H NMR spectra of LiN(SiHMe₂)tBu ($\delta_{\text{SiH}} 4.49$ ppm)⁵¹ and LiN(SiHMe₂)₂ ($\delta_{\text{SiH}} 4.49$ ppm)³⁰ appeared at frequencies lower than those in spectra of their respective silazanes. The $^1\text{J}_{\text{SiH}}$ were systematically smaller for the lithium silazido than for the corresponding arylsilazanes. The IR spectra of these compounds (KBr) contained signals at 2069 cm^{-1} (**2a**), 2056 cm^{-1} (**2b**), and 1981 and 2022 cm^{-1} (**2c**) assigned to the ν_{SiH} vibration, also at wavenumber lower than those for their silazane precursors.

Synthesis and Characterization of Rare-Earth Silazido Compounds.

Salt metathesis reactions of rare-earth chlorides and 3 equiv of **2a** in THF afford Ln{N(SiHMe₂)Ph}₃(THF)₂ (Ln = Sc (**3a**), Y (**4a**), Lu (**5a**); eq 3) in moderate yields after



extraction with benzene. Two THF molecules are coordinated to the rare-earth center in all three complexes. Attempts to prepare THF-free species by reactions of THF-free rare salts in benzene, toluene, or diethyl ether did not provide isolable products.

The ^1H NMR spectra of **3a–5a** revealed equivalent silazido ligands and equivalent THF ligands, present in a 3:2 ratio. The ^1H NMR resonances assigned to the Si–H moieties appeared at 5.24 ppm (**3a**, $^1\text{J}_{\text{SiH}} = 175.9$ Hz), 4.95 ppm (**4a**, $^1\text{J}_{\text{SiH}} = 173.2$ Hz), and 4.90 ppm (**5a**, $^1\text{J}_{\text{SiH}} = 173.6$ Hz). The high $^1\text{J}_{\text{SiH}}$ values indicated that the silazido ligands contained classical, two-center–two-electron (2c-2e) Si–H groups rather than bridging Ln–H–Si. The apparent equivalence of the silazido ligands was maintained in a ^1H NMR spectrum of **4a** acquired at 194 K in toluene-*d*₈, which contained only one Si–H resonance at 5.11 ppm. Each compound's IR spectrum (KBr)

gave results at odds with this picture of highly symmetrical molecules in solution. Two high frequency modes ($>2000\text{ cm}^{-1}$) were observed at 2113 and 2064 cm^{-1} for **3a**, at 2117 and 2075 cm^{-1} for **4a**, and at 2123 and 2081 cm^{-1} for **5a**. These two bands were assigned to the ν_{SiH} vibrations of inequivalent but classically bonded $\text{N}(\text{SiHMe}_2)\text{Ph}$ ligands in the compounds, on the basis of the X-ray diffraction studies below.

The molecular structures of **3a** (two independent molecules in the unit cell), **4a**, and **5a** (one molecule per unit cell) adopt similarly distorted trigonal bipyramidal geometries with two pseudoaxial THF and three equatorial silazido ligands. As a representative example, the ScN_3 core is planar ($\sum_{\text{NScN}} = 360^\circ$) and the axial THF O1-Sc1-O2 angle is $170.59(8)^\circ$ in **3a** (Figure 1). None of the structures contain close contacts

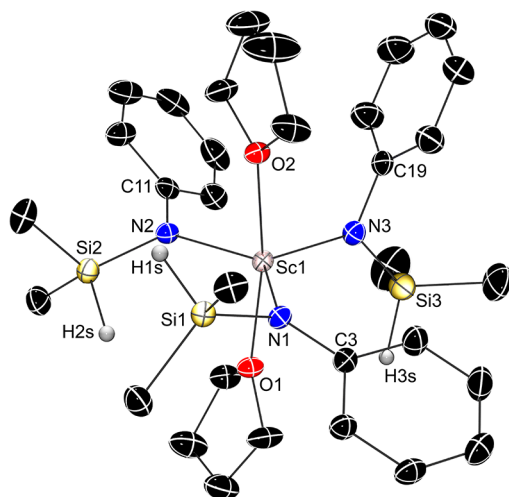
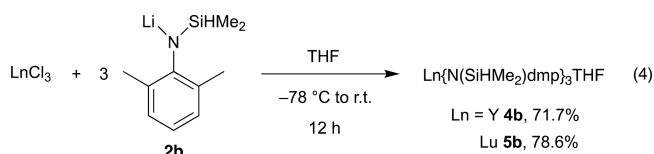


Figure 1. Thermal ellipsoid plot of $\text{Sc}\{\text{N}(\text{SiHMe}_2)\text{Ph}\}_3(\text{THF})_2$ (**3a**), with ellipsoids illustrated at 35% probability. Only one of the two independent molecules is included in the image. The only H atoms shown are those bonded to silicon centers, which were found objectively and refined using a riding model. Selected interatomic distances (Å): Sc1-N1 , 2.142(2); Sc1-N2 , 2.137(2); Sc1-N3 , 2.077(2); Si1-H 1s , 1.42(3); Si2-H 2s , 1.44(3); Si3-H 3s , 1.44(3). Selected interatomic angles (deg): N1-Sc1-N2 , 129.86(9); N2-Sc1-N3 , 114.86(9); N3-Sc1-N1 , 115.27(9); O1-Sc1-O2 , 170.59(8); Sc1-N1-Si1 , 114.5(1); Sc1-N2-Si2 , 118.5(1); Sc1-N3-Si3 , 126.6(1).

between the rare-earth center and the SiH moiety (i.e., structural features typically attributed to $\text{Ln}\leftarrow\text{H-Si}$ are not observed), which is consistent with the NMR and IR spectroscopic data. Two of the planar silazido ligands are approximately coplanar with the LnN_3 plane of the trigonal-bipyramidal molecules, whereas the plane of the third ligand is orthogonal to the LnN_3 plane. In **3a** for example, the first two silazido planes (defined by the points at N1, Si1, C3 or N2, Si2, C11) and the scandium plane (defined by Sc1, N2, and N3) intersect with angles of 13.9 or 22.9° , while the angle of intersection with the third silazido plane (defined by N3, Si3, and C19) is 81.6° . The structural parameters of N1- and N2-based silazido ligands are also distinct from those of the N3 ligand. For example, the Sc1-N1 and Sc1-N2 distances (2.142(2) and 2.137(2) Å) are longer than the Sc1-N3 distance (2.077(2) Å) of the orthogonally oriented ligand. These features extend to the other independent scandium

molecule in the unit cell of **3a** and yttrium **4a** and lutetium **5a** analogues.

Salt metathesis reactions of the yttrium and lutetium chlorides and 3 equiv of $\text{LiN}(\text{SiHMe}_2)\text{dmp}$ (**2b**) provide $\text{Ln}\{\text{N}(\text{SiHMe}_2)\text{dmp}\}_3\text{THF}$ ($\text{Ln} = \text{Y}$ (**4b**), Lu (**5b**); eq 4) in good yields. Unfortunately, the synthesis of the scandium analogue was not successful, and instead the reaction afforded the free amine.



The synthesis of these two compounds required THF as the solvent, as was observed for the phenyl-based ligands above. Integration of the ^1H NMR spectra of **4b** and **5b** revealed that only one molecule of THF coordinated to the metal center, likely a result of the more sterically hindered 2,6-dimethylphenyl-substituted silazido ligands in comparison to the phenyl-substituted **3a**, **4a**, and **5a**. The ^1H NMR spectra suggested that **4b** and **5b** each also contained three equivalent silazido ligands. The signals assigned to SiH groups in the ^1H NMR spectra, acquired at room temperature, showed smaller coupling constants for **4b** (5.20 ppm, $^1J_{\text{SiH}} = 151.3\text{ Hz}$) and **5b** (5.20 ppm, $^1J_{\text{SiH}} = 155.8\text{ Hz}$) than for **3a-5a**. These 2,6-dimethylphenylsilazido compounds were fluxional, but the exchange was not resolved in ^1H NMR spectra of **4b** and **5b** acquired at 191.5 K, which showed a flat region and a broad, very low intensity signal, respectively, in the region expected for the SiH resonance. Infrared spectra (KBr) contained moderate-intensity and weak-intensity signals in the $\nu_{\text{Si-H}}$ region of **4b** at 2057 and 1966 cm^{-1} and **5b** at 2071 and 1902 cm^{-1} for nonbridging and bridging interactions, respectively. Together, these data suggest that the Si-H moieties form bridging interactions with the metal center, and weakly and strongly interacting SiH groups undergo fast exchange on the NMR time scale to give an averaged signal with a moderate coupling constant at room temperature.

Single-crystal X-ray diffraction reveals that, although both **4b** and **5b** contain four-coordinate $\text{Ln}\{\text{N}(\text{SiHMe}_2)\text{dmp}\}_3\text{THF}$ species, the conformations of the solid-state structures are different. The three similarly bonded ligands in the yttrium compound **4b** each form a bridging $\text{Y}\leftarrow\text{H-Si}$ interaction (Figure 2), whereas the lutetium compound **5b** contains only two $\text{Lu}\leftarrow\text{H-Si}$ interactions (Figure 3). The Y-N interatomic distances (2.233 Å) are equivalent within error, and the N-Y-N and N-Y-O angles ($110 \pm 1^\circ$) are close to those of an ideal tetrahedron. Despite small differences, the three ligands are related by approximate C_3 symmetry (ignoring the orientation of the THF), with the SiHMe_2 groups all pointing counterclockwise when the molecule is viewed down the O1-Y1 vector. In addition, the SiH groups are also directed toward the THF ligand, while the aryl groups point away from the THF ligand.

The lutetium analogue **5b** (Figure 3), in contrast, contains three inequivalently bonded silazido ligands with long (Lu1-N1 , 2.202(3) Å), medium (Lu1-N2 , 2.193(3) Å), and short (Lu1-N3 , 2.179(3) Å) metal-nitrogen distances (the longest and shortest bonds are statistically different on the basis of a comparison of 3σ). Moreover, the ligand with the shortest

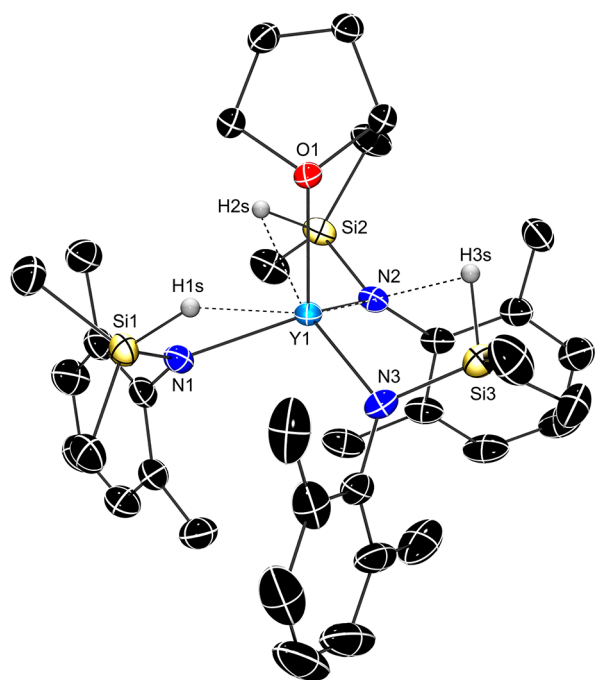


Figure 2. Thermal ellipsoid plot of $Y\{N(SiHMe_2)dmp\}_3THF$ (**4b**), with ellipsoids illustrated at 35% probability. H atoms bonded to Si were located in the Fourier difference map, were refined anisotropically, and are included in the illustration. All other H atoms were placed in calculated positions and are not shown for clarity. Selected interatomic distances (Å): Y1–N1, 2.233(2); Y1–N2, 2.235(2); Y1–N3, 2.235(3); Y1–H1s, 2.62(3); Y1–H2s, 2.69(3); Y1–H3s, 2.89(4); Si1–H1s, 1.45(3); Si2–H2s, 1.39(2); Si3–H3s, 1.45(4). Selected interatomic angles (deg): N1–Y1–N2, 110.74(9); N2–Y1–N3, 109.81(9); N3–Y1–N1, 111.01(9); O1–Y1–N1, 111.12(8).

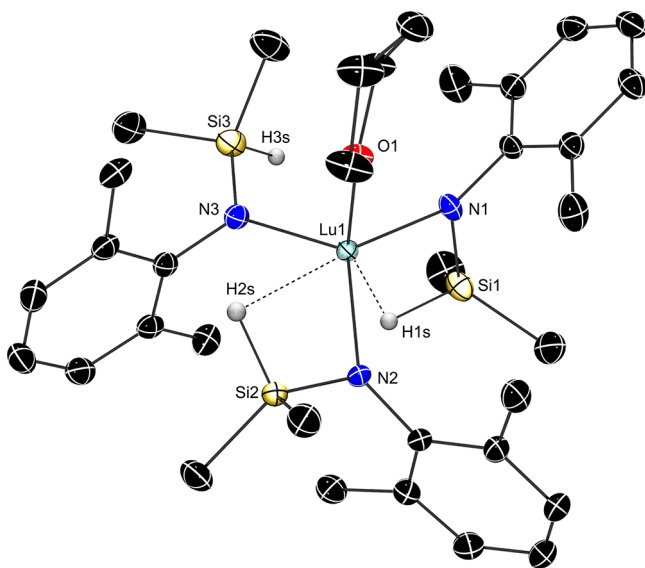
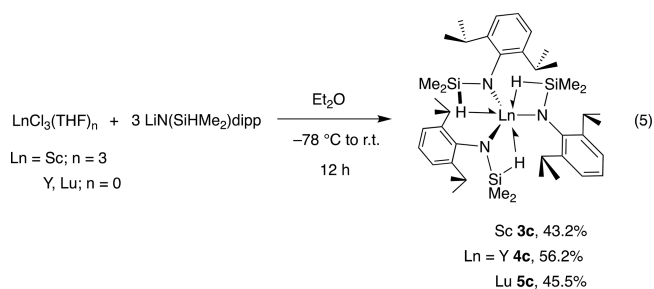


Figure 3. Thermal ellipsoid plot of $Lu\{N(SiHMe_2)dmp\}_3THF$ (**5b**), with ellipsoids illustrated at 35% probability. Selected interatomic distances (Å): Lu1–N1, 2.202(3); Lu1–N2, 2.194(3); Lu1–N3, 2.179(3); Lu1–H1s, 2.32(5); Lu1–H2s, 2.73(4); Si1–H1s, 1.40(2); Si2–H2s, 1.400(7); Si3–H3s, 1.40(3). Selected interatomic angles (deg): N1–Lu1–N2, 116.9(1); N2–Lu1–N3, 120.1(1); N3–Lu1–N1, 108.8(1); O1–Lu1–N1, 98.0(1).

distance between Lu and Si atoms (i.e., Lu1...Si1, 2.997(1) Å) and the smallest angle to silicon (Lu1–N1–Si1, 99.2(1)°) is

the one with the longest Lu–N distance. The N–Lu–N angles vary considerably from those of an ideal tetrahedron (N1–Lu1–N2, 116.9(1); N1–Lu1–N3, 108.8(1); N2–Lu1–N3, 120.1(1)°), and the amidos bond to lutetium to give a LuN₃ core that also is not planar ($\sum_{NLuN} = 345.8^\circ$). Instead of approximate C₃ symmetry, the N1 silazido ligand is oriented with its bridging Lu←H–Si pseudo-*trans* to the THF ligand, and its aryl group points toward the THF. Thus, **4b** and **5b**, which appear very similar in spectroscopic features, crystallize with distinct structures.

Salt metathesis reactions of rare-earth chlorides and $LiN(SiHMe_2)dipp$ provide the homoleptic species $Ln\{N(SiHMe_2)dipp\}_3$ in moderate yields ($Ln = Sc$ (**3c**), Y (**4c**), Lu (**5c**); eq S).⁴² Fortunately, and in contrast to the THF



solvent required for syntheses of **3a–5a** and **4b** and **5b**, the salt metathesis reactions of **2c** proceed in diethyl ether at low temperature. The crude products were recrystallized in pentane to provide analytically pure **3c–5c**.

The ¹H NMR spectra of **3c–5c** contained one set of signals for the silazido ligand, which indicated that the three ligands were equivalent or were undergoing rapid exchange in solution at room temperature. The ¹H NMR resonances assigned to the Si–H groups appeared at 5.43 ppm (**3c**, ¹J_{SiH} = 142.6 Hz), 5.17 ppm (**4c**, ¹J_{SiH} = 129.2 Hz), and 5.43 ppm (**5c**, ¹J_{SiH} = 127.6 Hz), which suggested that these compounds contain Ln←H–Si bridging interactions. Most significantly, the Si–H signal of **4c** at 5.17 ppm correlated with the yttrium resonance at 378.5 ppm in a ¹H–⁸⁹Y HSQC experiment (measured at room temperature), which also provided evidence for covalent, nonclassical interactions between SiH groups and the metal center.⁴² In addition, the SiMe signal was correlated in ¹H–¹⁵N HMBC experiments to provide ¹⁵N NMR chemical shifts of 160.9 (**3c**), 142.3 ppm (**4c**), and 140.3 ppm (**5c**) signals.

The compounds **3c–5c** are fluxional. The ¹H NMR spectrum of the scandium complex **3c**, acquired at 213 K, contained three resonances at 5.55, 5.44, and 5.24 ppm assigned to three inequivalent Si–H groups (Figure 4). Similarly, the spectrum of **4c** obtained at 205 K contained three signals at 5.41 ppm (¹J_{SiH} = 131.9 Hz), 5.26 ppm (¹J_{SiH} = 140.7 Hz) and 4.89 ppm (¹J_{SiH} = 115.8 Hz) assigned to the Si–H moieties. 129.5 Hz, the average of these values, matches the value measured at room temperature for **4c** under fast exchange. In addition, six multiplets were assigned to methine protons of dipp groups. The low-temperature ¹H NMR spectrum of **5c**, acquired at 215 K, contained only two resonances at 5.58 ppm (1 H) and 5.33 ppm (2 H), with the latter signal assigned to coincident SiH chemical shifts (Figure 5). A ¹H–²⁹Si HMQC spectrum of **5c**, acquired at 215 K (decoupling off), contained three signals at –29.73, –29.07, and –26.60 ppm in the ²⁹Si dimension that correlated with

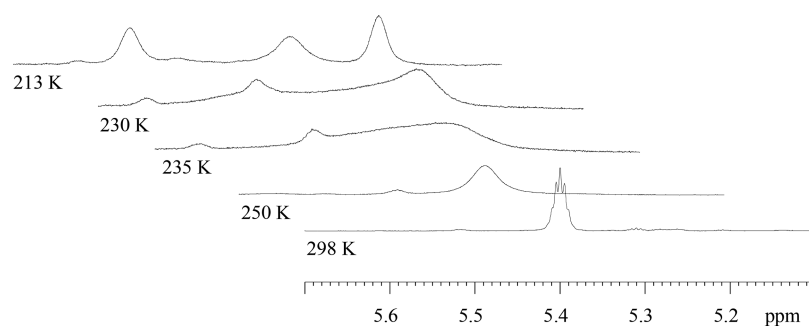


Figure 4. Stack plot of ^1H NMR spectra of **3c**, measured from 298 to 213 K in toluene- d_8 .

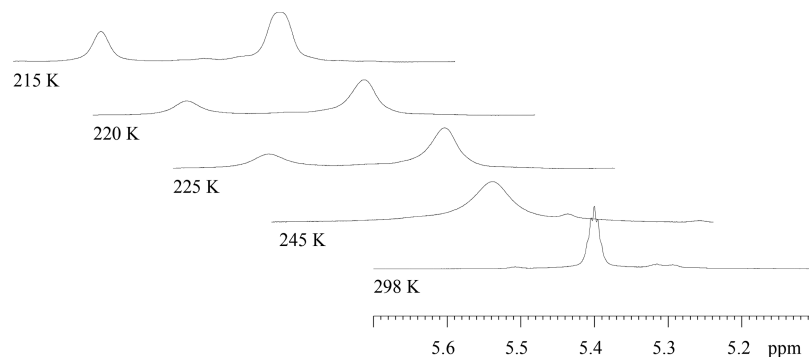


Figure 5. Stack plot of ^1H NMR spectra of **5c**, measured from 298 to 215 K in toluene- d_8 .

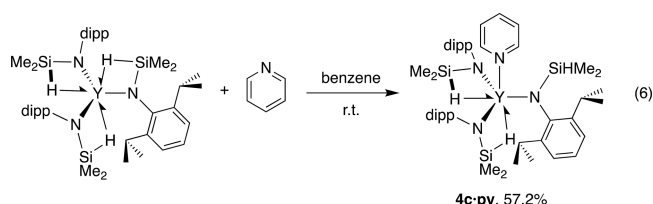
signals at 5.58 ppm ($^1J_{\text{SiH}} = 133.1$ Hz), 5.33 ppm ($^1J_{\text{SiH}} = 138.5$ Hz), and 5.33 ppm ($^1J_{\text{SiH}} = 111.8$ Hz), respectively (Figure 6). Together, these observations indicate that the three ligands of **3c–5c** are inequivalent in the solution-phase low-temperature structure and are undergoing exchange. An EXSY experiment on compound **4c**, acquired at 205 K, confirmed the SiH exchange (Figure 7).

The IR spectra contained bands in the $\nu_{\text{Si-H}}$ region at 2046 and 1908 cm^{-1} for **3c**, 1934 and 1883 cm^{-1} for **4c**, and 1942 and 1877 cm^{-1} for **5c**. The lower energy signal is more intense than the higher energy band, suggesting that the bridging moieties with (relatively) strong metal–hydrogen bonds are most prevalent in the structure.

Single-crystal X-ray diffraction studies reveal that both independent molecules in all of the structures of compounds **3c**,⁴² **4c**, and **5c** adopt a low-symmetry, planar geometry ($\sum_{\text{NLnN}} \approx 360^\circ$). Two of the dipp groups are located above the LnN_3 plane, while the third is located below the LnN_3 plane. This conformation, as well as the metrical parameters (Ln-N and Ln-H distances and $\angle\text{N-Ln-N}$ and $\angle\text{Ln-N-Si}$ angles) highlight the inequivalence of ligands in **3c–5c**. For example, the Y1-N2 distance in **4c** (Figure 8) is longer, the Y-H2s distance is shorter, and the Y-N2-Si2 angle is smaller than in the other two ligands (N1 and N3). Although the \sum_{NYN} values for the two independent molecules of **4c** are 358 and 359° , the $\angle\text{N1-Y1-N3}$ angle (opposite to the longer Y1-N2 bond) is much larger (130°) than the other two $\angle\text{N-Y-N}$ angles ($\sim 115^\circ$, opposite to the shorter bonds). Even though the ligands are inequivalent, the interatomic distances and angles for all of the ligands of **4c** and **5c** provide evidence for Ln-H-Si interactions, as shown in Figure 8. In addition to the three Ln-H-Si secondary interactions in each compound, the short distances between the rare-earth center and one of the methine CH groups in **3c** (Sc1-H40 , 2.34(3)

Å), **4c** (Y1-H27A , 2.37(4) Å), and **5c** (Lu1-H40A , 2.34(6) Å) respectively suggest that agostic bonds are also present.

Addition of 1 equiv of pyridine to **4c** in benzene provides the adduct $\text{Y}\{\text{N}(\text{SiHMe}_2)\text{dipp}\}_3\cdot\text{NC}_5\text{H}_5$ (**4c·py**, eq 6), which



was recrystallized from pentane. 4-(*N,N*-dimethylamino)pyridine (dmap) also coordinates to **4c** to give **4c·dmap**, although this species was not isolated. Evidence for dmap coordination includes a deshielded signal at 5.46 ppm, assigned to the SiH in the coordinated compound, in comparison to the value in **4c**. As in the precursor **4c**, all three silazido ligands in **4c·py** appeared to be equivalent in its ^1H NMR spectrum; however, the overall symmetry is lowered such that isopropyl of the dipp groups in **4c·py** provided two methyl signals, whereas the dipp methyls of **4c** appeared as a single doublet.

The ^1H NMR resonance at 5.33 ppm ($^1J_{\text{SiH}} = 150.5$ Hz) in a spectrum acquired at room temperature was assigned to the Si-H group of **4c·py**. The SiH is deshielded in **4c·py** relative to **4c**. The larger $^1J_{\text{SiH}}$ value of **4c·py** than that of **4c** suggests that the coordination of pyridine disrupts one of the Ln-H-Si bridging interactions; a structure containing two Ln-H-Si and one 2c-2e SiH is assigned on the basis of its estimated coupling of 153 Hz, calculated from the weighted average of $^1J_{\text{SiH}}$ for Ln-H-Si of 130 Hz and the value for 2c-2e one-bond Si-H scalar coupling of 200 Hz. The IR spectrum of **4c·py** supports this analysis; two bands in the $\nu_{\text{Si-H}}$ region at 2103

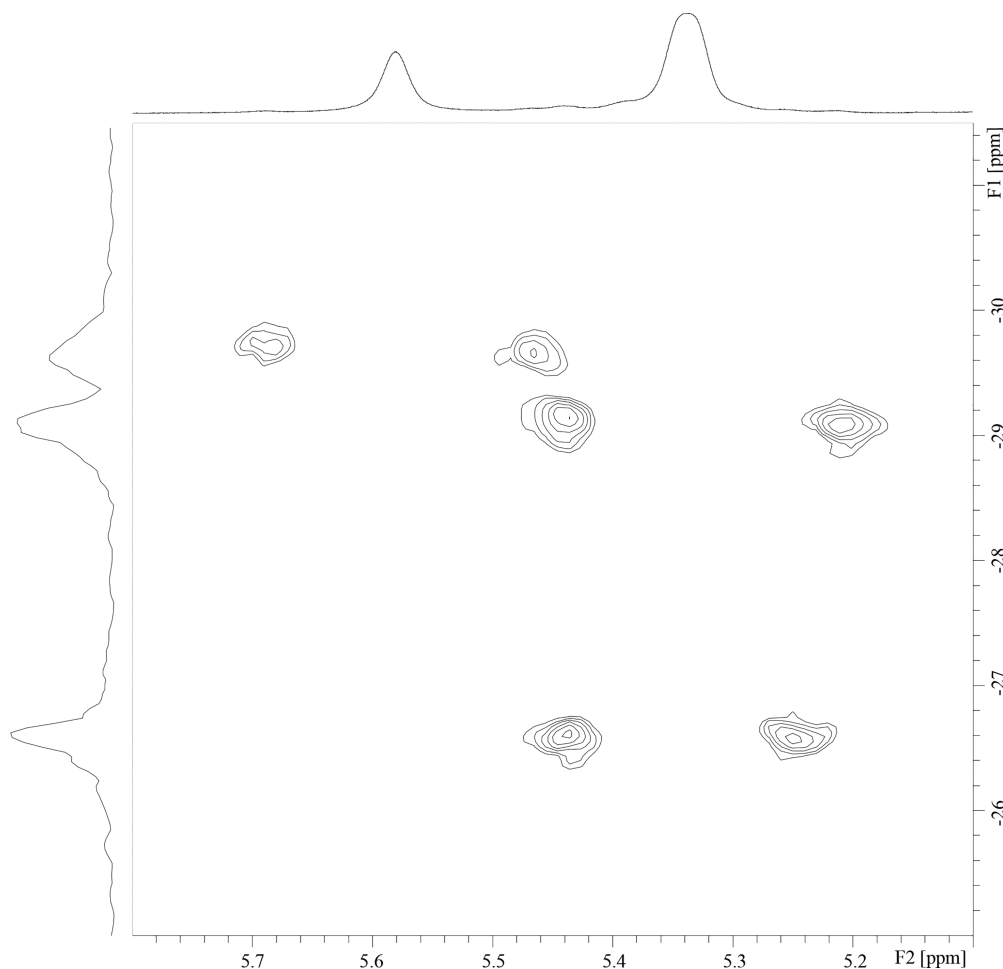


Figure 6. $^1\text{H}\{^{29}\text{Si}\}$ HMQC NMR spectrum of lutetium compound **5c** acquired at 215 K in toluene- d_8 . The corresponding 1D ^1H NMR spectrum is shown on top of the 2D spectrum.

and 1959 cm^{-1} indicate the presence of both classical and nonclassical SiH interactions with the metal center.

A single-crystal X-ray diffraction study confirms that pyridine is coordinated to the yttrium center in **4c**·py, that only two of the three silazido ligands form Y←H–Si interactions, and that $\angle\text{N–Y–N}$ angles associated with silazido ligands are smaller in **4c**·py than in **4c** (Figure 9). Remarkably, the nearly planar YN_3 core of **4c** is only slightly perturbed by pyridine coordination ($\sum_{\text{N–Ln–N}} \approx 349^\circ$) vs 359° in **4c**, whereas the three angles around YN_3 in THF-coordinated **4b** sum to 331.5° . The Y–H interatomic distances and $\angle\text{Y–N–Si}$ angles of N1- and N2-based ligands suggest Y←H–Si interactions, whereas the silazido ligand associated with N3 appears to be classically bonded.

Ketone Hydrosilylation Reactions with $\text{Ln}\{\text{N}(\text{SiHMe}_2)\text{-dipp}\}_3$. Reactions of the series of compounds $\text{Ln}\{\text{N}(\text{SiHMe}_2)\text{-Ph}\}_3(\text{THF})_2$, $\text{Ln}\{\text{N}(\text{SiHMe}_2)\text{dmp}\}_3\text{THF}$, and $\text{Ln}\{\text{N}(\text{SiHMe}_2)\text{dipp}\}_3$ and the ketones acetone, acetophenone, and benzophenone probe the reactivity of the bridging Ln←H–Si and Ln–N bonds in silazido moieties as a function of steric properties of the silazido, the presence, number, and nature of donor ligands, the steric properties of the carbonyl, and its reactivity as an electrophile or as a weak acid. In our initial communication, we reported that **4c** and acetophenone react rapidly (<3 min, -78°C) to give $\text{Y}\{\text{N}(\text{SiMe}_2\text{OCHMePh})\text{-dipp}\}\{\text{N}(\text{SiHMe}_2)\text{dipp}\}_2$, formed by formal addition of one Si–H across the acetophenone C=O.

The attempts to react $\text{Ln}\{\text{N}(\text{SiHMe}_2)\text{Ph}\}_3(\text{THF})_2$ or $\text{Ln}\{\text{N}(\text{SiHMe}_2)\text{dmp}\}_3\text{THF}$ with ketones did not afford isolable products yet offered an important contrast with $\text{Ln}\{\text{N}(\text{SiHMe}_2)\text{dipp}\}_3$ and their hydrosilylated products. The reaction of $\text{Lu}\{\text{N}(\text{SiHMe}_2)\text{Ph}\}_3(\text{THF})_2$ with 1 equiv (or excess) of benzophenone gives free THF, all of **5a** is consumed, but multiple unknown species are formed. ^1H – ^{13}C HSQC experiments on the reaction mixture did not provide evidence for hydrosilylation (as observed in **4c**–**5c** below).

The reaction of $\text{Ln}\{\text{N}(\text{SiHMe}_2)\text{dmp}\}_3\text{THF}$ (**4b**, **5b**) with 1 equiv of acetophenone also yielded multiple products, including $\text{Ln}\{\kappa^2\text{-N}(\text{SiMe}_2\text{OCHMePh})\text{dmp}\}_n\{\text{N}(\text{SiHMe}_2)\text{-dmp}\}_{3-n}$. These products were characterized by the presence of multiple SiH and CH ^1H NMR signals from 5.0 to 5.5 ppm, which were assigned by 2D heteronuclear NMR experiments. Unfortunately, **4b** and **5b** starting materials were also present in the reaction mixture, and the hydrosilylation products could not be isolated. Likewise, the reactions of **4b** or **5b** with benzophenone (1–5 equiv) formed mixtures of one, two, and (possibly) three ketone-inserted products, but the species decomposed during attempted isolation.

In contrast, reactions of diisopropylaniline-substituted silazido compounds and ketones are rapid, are selective, and give isolable products. **4c** and **5c** rapidly react with either acetophenone or benzophenone to give silyl ether-containing

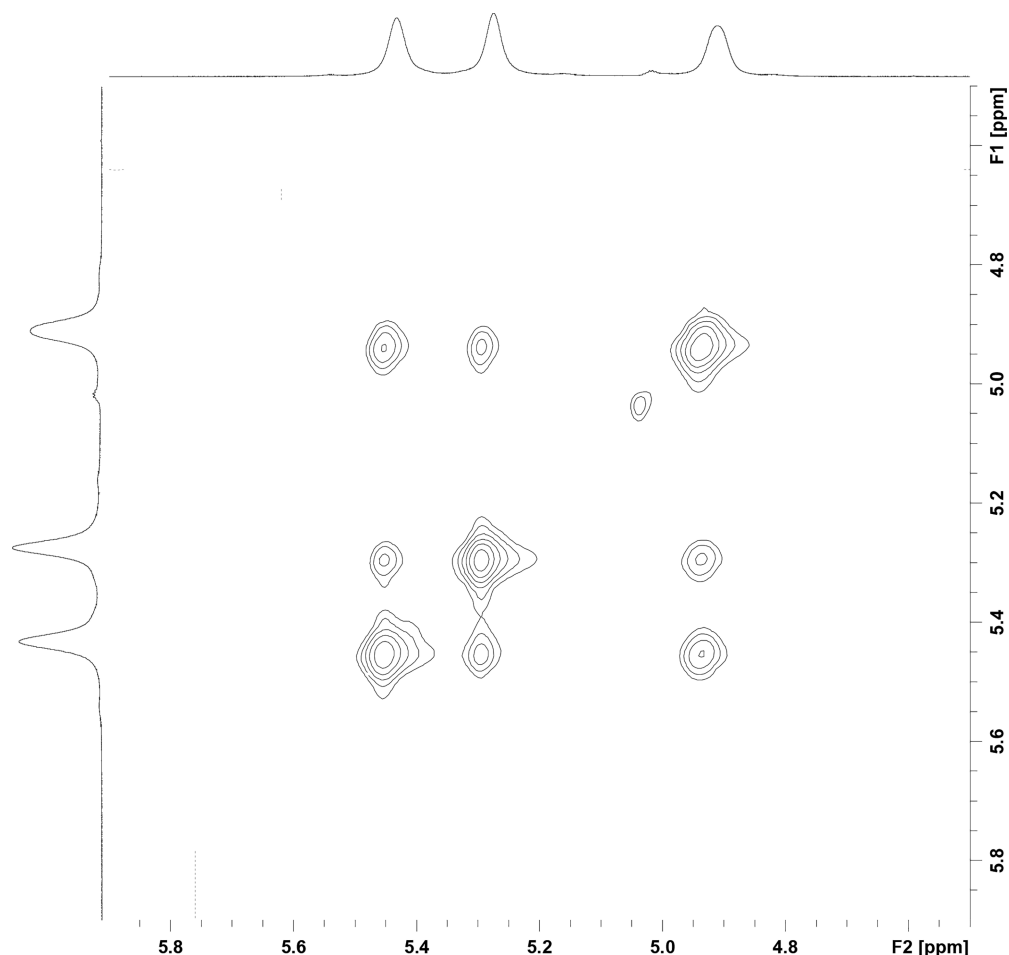
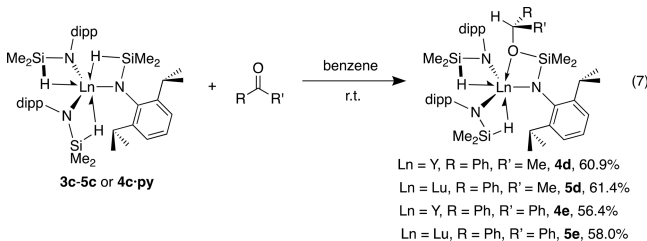


Figure 7. ^1H EXSY NMR spectrum of **4c** obtained at 205 K in toluene- d_8 .

heteroleptic silazido compounds of the type $\text{Ln}\{\kappa^2\text{-N}(\text{SiMe}_2\text{OCHRR}')\text{dipp}\}\{\text{N}(\text{SiHMe}_2)\text{dipp}\}_2$ (eq 7; R, R' =



Ph, Me, Ln = Y (**4d**), Ln = Lu (**5d**); R, R' = Ph, Ph, Ln = Y (**4e**), Ln = Lu (**5e**)). These reactions are remarkably rapid, and even reactions performed at -78°C in toluene- d_8 and measured by ^1H NMR at that temperature show quantitative conversion within 3 min to the product ($\sim 60\%$ isolated yield after crystallization). These products also form quantitatively in reactions performed at room temperature. Remarkably, the pyridine-coordinated complex **4c**·py also reacts instantaneously with acetophenone to give the hydrosilylated product **4d** and noncoordinated pyridine.

Key NMR and IR spectroscopic data for the carbonyl-inserted products are given in Table 2. A ratio of 2:1 was observed for the integrals of two equivalent SiH groups to one new CH group in the ^1H NMR spectrum. The signal assigned to that CH group appeared as a multiplet in acetophenone-inserted compounds (**4d** and **5d**), while the CH group

appeared as a broad singlet in benzophenone-inserted compounds (**4e** and **5e**). Furthermore, correlations in ^1H - ^{13}C HMQC (one-bond) experiments between the new CH group and the methine carbon of the silyl ether, which appeared at a characteristic chemical shift of ~ 80 ppm, also provide evidence for SiH addition to the ketone. The remaining SiH moieties form bridging $\text{Ln}\leftarrow\text{H}\text{-Si}$ bonds, characterized on the basis of values of $^1J_{\text{SiH}}$ and ν_{SiH} . We also note a significant change in ^{29}Si NMR chemical shift of the silyl ether (~ 3 ppm), whereas the SiHMe_2 group appeared at ca. -25 ppm.

Single-crystal X-ray diffraction studies of all four compounds confirm that the ketone hydrosilylation gives one silyl ether containing silazido ligand and two silazido ligands with bridging $\text{Ln}\leftarrow\text{H}\text{-Si}$ interactions (see, for example, $\text{Y}\{\kappa^2\text{-N}(\text{SiMe}_2\text{OCHPh}_2)\text{dipp}\}\{\text{N}(\text{SiHMe}_2)\text{dipp}\}_2$ (**4e**) in Figure 10). The coordination geometry of the LnN_3O core is best described as a trigonal monopyramid, rather than a tetrahedron as in $\text{Y}\{\text{N}(\text{SiHMe}_2)\text{dmp}\}_3\text{THF}$ (**4b**). For example, the sum of N-Ln-N angles for the three silazido ligands (\sum_{NLnN}) is $356.14\text{--}357.43^\circ$ in all four complexes.

With acetophenone and benzophenone, only single addition products proved isolable. The reaction of 3 equiv of acetophenone and **4c** or **5c** generates $\text{HN}(\text{SiHMe}_2)\text{dipp}$, likely resulting from deprotonation of acetophenone, along with a multitude of unidentified rare-earth-containing products. The 3 equiv of the nonenolizable ketone, benzophenone, and **4c** or **5c** react to give only the corresponding

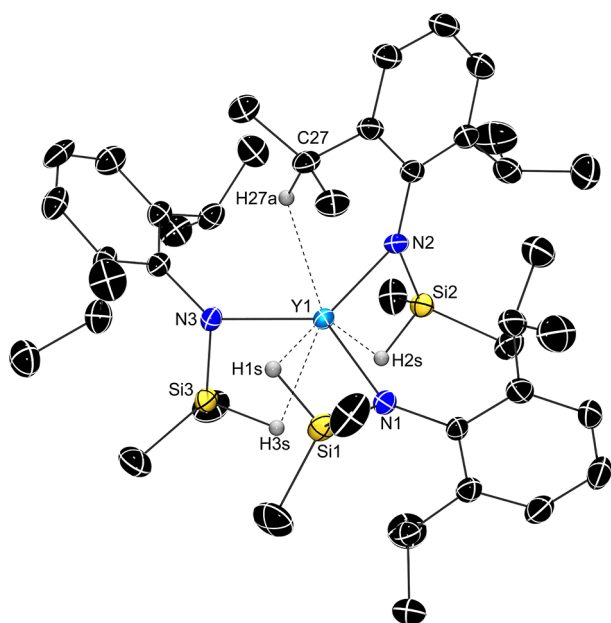
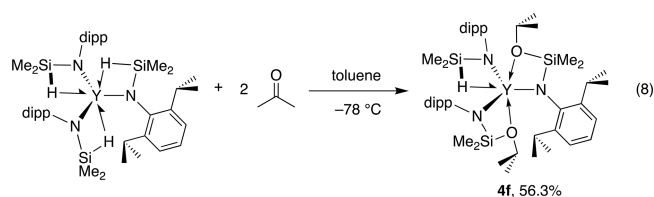


Figure 8. Thermal ellipsoid plot of $Y\{N(SiHMe_2)dipp\}_3$ (**4c**; CCDC 1838233), with ellipsoids illustrated at 35% probability. H atoms bonded to Si were located in the Fourier difference map, were refined anisotropically, and are included in the illustration. All other H atoms are not shown for clarity. Selected interatomic distances (Å): Y1–N1, 2.247(3); Y1–N2, 2.293(3); Y1–N3, 2.251(3); Y1–H1s, 2.50(5); Y1–H2s, 2.24(4); Y1–H3s, 2.43(4); Si1–H1s, 1.37(6); Si2–H2s, 1.38(4); Si3–H3s, 1.53(4). Selected interatomic angles (deg): N1–Y1–N2, 113.4(1); N2–Y1–N3, 114.2(1); N3–Y1–N1, 130.0(1); Y1–N1–Si1, 102.4(1); Y2–N2–Si2, 94.2(2); Y3–N3–Si3, 101.4(1)°. $Sc\{N(SiHMe_2)dipp\}_3$ (**3c**) analogue, CCDC 1838231; $Lu\{N(SiHMe_2)dipp\}_3$ (**5c**) analogue, CCDC 1838230.

monoaddition products **4e** and **5e**, and the excess benzophenone does not undergo additions to **4e** or **5e**. This lack of further hydrosilylation may be attributed to the steric effects of bulky diisopropylphenylsilazido ligands or the electronic effect of the coordinated silyl ether in **4e** or **5e** that diminished the Lewis acidity of the rare-earth center. In this context, we note that similar compounds $Ln\{N(SiHMe_2)dmp\}_3 \cdot THF$ (**4b** and **5b**), which also contain a LnN_3O first coordination sphere and two or three $Ln \leftarrow H-Si$ interactions, reacts with ketones via hydrosilylation but does not provide isolable or long-lived products. Likely, this behavior results from the dimethylphenylsilazido ligands reacting via both hydrosilylation and protonolysis to give mixtures.

Acetone, representing smaller, easily enolized ketones, was allowed to react with **4c** in order to distinguish steric vs electronic effect based limitations on second additions. The reactions of 2–5 equiv of acetone and **4c** at room temperature in benzene provides mixtures of double- and triple-addition products, although the latter is only tentatively assigned and could not be isolated. This selectivity is similar in reactions performed at -78 °C in toluene. Fortunately, the product $Y\{\kappa^2-N(SiMe_2OCHMe_2)dipp\}_2\{N(SiHMe_2)dipp\}$ (**4f**) could be isolated (eq 8) after washing the reaction mixture with pentane to remove $Y\{\kappa^2-N(SiMe_2OCHMe_2)dipp\}_3$.

The 1H NMR spectrum of **4f** revealed two doublets at 0.48 and 0.34 ppm (3 H each) and a broad signal at 5.57 ppm for one $SiHMe_2$ group (1 H). Although this $Si-H$ signal appeared at high frequency, its one-bond coupling constant ($J_{SiH} = 138.1$ Hz) suggested that it was part of a bridging $Y \leftarrow H-Si$



structure. One set of signals was assigned to the dipp group in this ligand, including two isopropyl groups that show hindered rotation. Integration of two singlets for $SiMe_2OCHMe_2$ at 0.32 and 0.23 ppm (6 H each) indicated that two of these groups were formed. One signal at 4.17 ppm (2 H) was assigned to the methine CH group of $SiOCHMe_2$, which indicates that the two siloxane-containing silazido ligands were equivalent. This signal correlated in a COSY experiment to doublets at 0.88 and 0.84 ppm (6 H each) assigned to the methyl groups. Resonances assigned to two isopropyl groups of the dipp indicated that there was also hindered rotation around the N–C bond in these ligands. The isopropyl groups from dipp and $OCHMe_2$ were distinguished in a COSY experiment. In addition, the silyl ether carbon ^{13}C NMR resonance at 71.33 ppm correlated to the signal in the proton at 4.17 ppm assigned to $OCHMe_2$ in a $^1H-^{13}C$ HMQC experiment and to the doublets at 0.88 and 0.84 ppm in a $^1H-^{13}C$ HMBC experiment. These cross peaks unambiguously assign these signals as a part of $OCHMe_2$. The $^{13}C\{^1H\}$ NMR spectrum, however, contained a multitude of signals at ca. 25 ppm corresponding to isopropyl groups from dipp and $OCHMe_2$.

The two ^{29}Si NMR resonances in a $^1H-^{29}Si$ HMQC experiment of **4f** appeared at 0.23 and -25.4 ppm, with the former providing evidence for $Si-O$ bond formation. In addition, the IR spectrum contained a signal at 1991 cm^{-1} assigned to the SiH group, which further suggested the formation of a $Y \leftarrow H-Si$ interaction in **4f**.

A single-crystal X-ray diffraction study of **4f** reveals that the five-coordinate metal center is distorted trigonal bipyramidal (Figure 11), similarly to **3a–5a**, with O1 and O2 occupying axial sites ($O1-Y1-O2$, $157.61(6)^\circ$). The N1, N2, and N3 in **4f** are equatorial, adopting a planar geometry around the yttrium center ($\sum_{NLnN} = 359.91(6)^\circ$). Only the $\angle N2-Y1-N3$ angle ($125.42(6)^\circ$) is larger than 120° , while the other two $\angle N-Y-N$ angles are less than 120° . Even though two oxygens are coordinated from the two silyl ethers, the yttrium center remains sufficiently electrophilic to form a secondary $Y \leftarrow H-Si$ interaction with the only silicon hydride present, which is positioned in the largest $\angle N2-Y1-N3$ angle of the equatorial plane. For comparison, five-coordinate **3a–5a** are also trigonal bipyramidal, with two THF and three silazido ligands, but do not form secondary interactions with any of the three SiH groups. Aside from the additional distortion of the axial ligands from trigonal-bipyramidal geometry in **4f** resulting from four-membered rings created by the chelating N,O silazido ligands, we also note that both N,O silazido ligands are oriented with the C, N, and Si plane orthogonal to the equatorial plane of the yttrium center. In contrast, only one of the three silazido ligands in **3a–5a** is orthogonal to the equatorial plane of the trigonal-bipyramidal metal center. Also, the unique SiH in **4f**, which forms a secondary interaction, is still reactive toward the hydrosilylation of acetone to give $Y\{\kappa^2-N(SiMe_2OCHMe_2)dipp\}_3$ (which unfortunately decomposed during isolation). Nonetheless, the reactivity of **4f** is distinct from that of **3a–5a**,

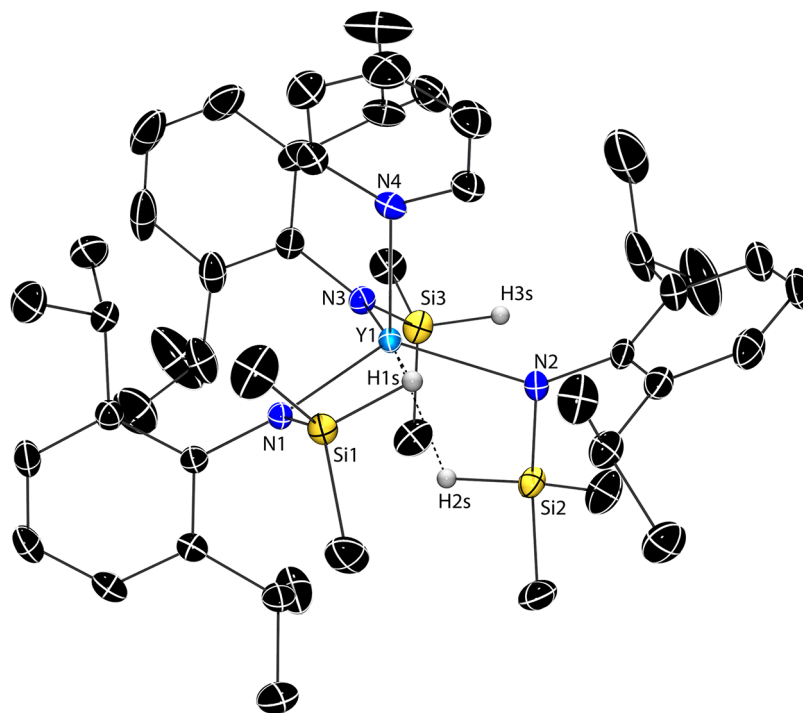


Figure 9. Thermal ellipsoid plot of $Y\{N(SiHMe_2)dipp\}_3 \cdot NC_5H_5$ (**4c·py**), with ellipsoids illustrated at 35% probability. H atoms bonded to Si were located in the Fourier difference map, were refined anisotropically, and are included in the illustration. All other H atoms are not shown for clarity. Selected interatomic distances (Å): Y1–N1, 2.249(2); Y1–N2, 2.286(3); Y1–N3, 2.261(2); Y1–N4, 2.455(3); Y1–H1s, 2.64(3); Y1–H2s, 2.47(4); Si1–H1s, 1.43(4); Si2–H2s, 1.36(4); Si3–H3s, 1.33(5). Selected interatomic angles (deg): N1–Y1–N2, 116.53(8); N2–Y1–N3, 113.91(9); N3–Y1–N1, 118.65(8).

Table 2. Key NMR and IR Spectroscopic Data of Carbonyl-Inserted Compounds

compound	^{13}C δ_{CH} (ppm)	1H δ_{CH} (ppm)	^{29}Si δ_{Si} (ppm)	1H δ_{SiH} (ppm)	$^1J_{SiH}$ (Hz)	IR (cm^{-1})
$Y\{\kappa^2-N(SiMe_2OCHPhMe)dipp\} \{N(SiHMe_2)dipp\}_2$ (4d)	77.46	5.00	3.94, –23.4	5.33	135.5	1997, 1891
$Lu\{\kappa^2-N(SiMe_2OCHPhMe)dipp\} \{N(SiHMe_2)dipp\}_2$ (5d)	78.09	5.06	3.46, nd	5.57	135.3	2001, 1881
$Y\{\kappa^2-N(SiMe_2OCHPh_2)dipp\} \{N(SiHMe_2)dipp\}_2$ (4e)	84.42	6.53	4.84, –24.1	5.01	131.9	1965, 1886
$Lu\{\kappa^2-N(SiMe_2OCHPh_2)dipp\} \{N(SiHMe_2)dipp\}_2$ (5e)	83.58	6.62	–4.10, –21.8	5.29	133.1	1957 br

whose reactivity with ketones does not provide convincing evidence of hydrosilylation.

The reaction between **3c–5c** or **4c·py** and the ketones is instantaneous even at -80 °C, and all attempts to monitor the transformation reveal the inserted products as the only spectroscopically detected species in reaction mixtures. Even coordinating ligands, such as excess pyridine (5 equiv), results in quantitative conversion faster than NMR- or cuvette-scale UV–vis (stopped-flow UV–vis experiments were limited by the air and moisture sensitivity of the silazido compounds). Thus, the mechanism of the hydrosilylation could not be directly probed through a rate law. Instead, the exchange of coordinated and noncoordinated pyridine in **4c·py** was investigated to determine the lability of pyridine and to confirm whether pyridine dissociates from **4c·py** prior to or subsequent to its reaction with ketones.

EXSY NMR experiments on mixtures of **4c** and pyridine (1.5 equiv) revealed cross peaks between coordinated and noncoordinated pyridine 1H NMR signals that were indicative of exchange. The rate constant for the exchange was determined by the integration of diagonal peaks and cross peaks over a series of mixing times (t_m).³² Measurement of the rate constant for exchange at 277 K revealed a fast process ($k = 5$ s $^{-1}$), while exchange at higher temperatures was too fast to be measured by EXSY. Rate constants were measured with two

different concentrations of pyridine down to 215 K ($k = 0.25$ s $^{-1}$) and two different concentrations of **4c·py**. The observed pseudo-first-order rate constants are independent of pyridine concentration but dependent on $[4c·py]$. We interpret this observation to result from dependence of the rate of exchange on the total amount of yttrium in solution, which is >99% in the form of **4c·py** (there is no pyridine-free **4c** detected). Thus, the extent of equilibrium and the rate of exchange between coordinated and noncoordinated pyridine will be independent of $[pyridine]$ in the presence of excess pyridine for both associative and dissociative processes. A plot of $\ln(k/T)$ vs $1/T$ provided the linearized temperature dependence of the rate constants (Figure 12). From this plot, the activation entropy ($\Delta S^\ddagger = -20(3)$ cal mol $^{-1}$ K $^{-1}$) and activation enthalpy ($\Delta H^\ddagger = 4.6(3)$ kcal mol $^{-1}$) rule out a dissociative process, which would be expected to show a positive entropy of activation and large enthalpy of activation. Instead, the data suggest an associative or interchange-type exchange process, which would require an open coordination site on yttrium. In **4c·py**, that site could be available without structural rearrangement or may displace one of the bridging Y–H–Si bonds.

We propose that an analogous coordination of the oxygen of a ketone to the rare-earth metal center is the first step in the pathway for the hydrosilylation reactions (Scheme 1). Note that, in the proposed mechanism for Lewis acid catalyzed

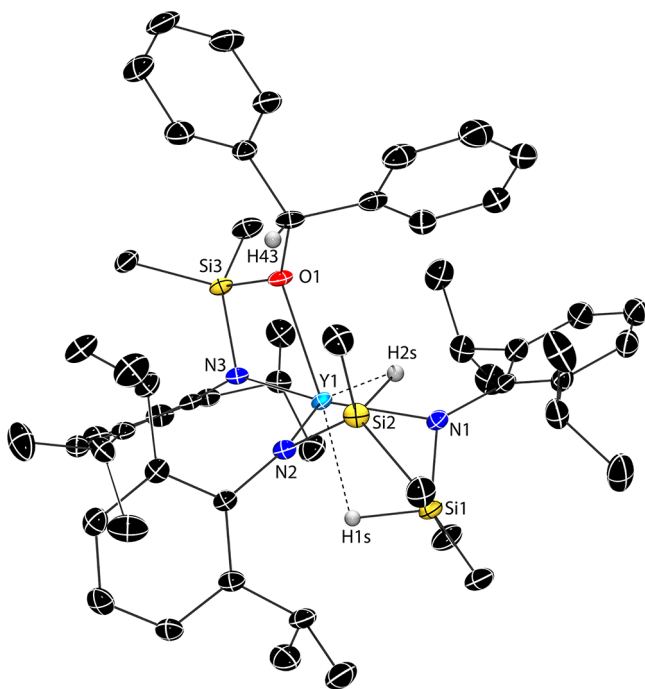


Figure 10. Thermal ellipsoid plot of $Y\{N(SiMe_2OCHPh_2)dipp\}\{N(SiHMe_2)dipp\}_2$ (**4e**), with ellipsoids illustrated at 50% probability. H atoms bonded to Si were located in the Fourier difference map, were refined anisotropically, and are illustrated. All other H atoms are not shown for clarity. Selected interatomic distances (Å): Y1–N1, 2.282(2); Y1–N2, 2.268(2); Y1–N3, 2.267(2); Y1–O1, 2.363(2); Y1–H1s, 2.42(3); Y1–H2s, 2.38(2); Si1–H1s, 1.47(2); Si2–H2s, 1.47(3). Selected interatomic angles (deg): N1–Y1–N2, 119.21(8); N2–Y1–N3, 118.96(8); N3–Y1–N1, 117.97(8); N1–Y1–O1, 103.89(7); N2–Y1–O1, 116.96(7); N3–Y1–O1, 66.19(7).

hydrosilylation of ketones, hydride abstraction by the Lewis acid is proposed as the first step rather than formation of the Lewis acid–ketone adduct.⁵³ In the reaction of $[Cp_2ZrN(SiHMe_2)_2]^+$ and carbonyls, zirconium was proposed to abstract the H from silicon concurrently with formation of the silicon–oxygen bond, on the basis of the reaction of $[Cp_2ZrN(SiHMe_2)_2]^+$ and dmap, which generates a *bona fide* terminal zirconium hydride.⁴⁰ In both of these examples, however, coordination of a carbonyl oxygen to the Lewis acid (metal) site cannot occur *cis* to metal–hydrogen bond formation. In contrast, **3c–5c** and **4c_{py}** contain one or two accessible, pseudoaxial sites *cis* to silazido ligands engaging secondary $Ln\leftarrow H-Si$ bonding, presumably facilitating the hydrosilylation.

CONCLUSION

Three series of rare-earth arylsilazido complexes, varying the steric properties of the aryl group and rare-earth center, provide five-coordinate bis(tetrahydrofuran) tris(silazido), four-coordinate mono(tetrahydrofuran) tris(silazido), and three-coordinate tris(silazido) pseudo-organometallic compounds. Fewer THF ligands are coordinated to rare-earth centers supported by larger, more sterically encumbered silazido ligands. The compounds containing fewer coordinated THF ligands instead contain more bridging $Ln\leftarrow H-Si$ bonding, with spectroscopic characteristics suggestive of weakened silicon–hydrogen bonds: namely, lowered Si–H stretching frequencies in the infrared spectra and lowered one-bond silicon–hydrogen coupling constants. In addition,

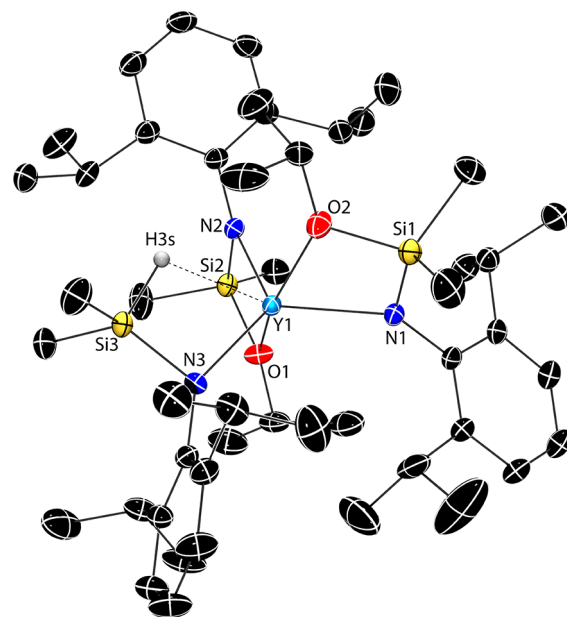


Figure 11. Thermal ellipsoid plot of $Y\{N(SiMe_2OCHMe_2)dipp\}_2\{N(SiHMe_2)dipp\}$ (**4f**), with ellipsoids illustrated at 35% probability. H atoms bonded to Si were located in the Fourier difference map, were refined anisotropically, and are illustrated. All other H atoms are not shown for clarity. Selected interatomic distances (Å): Y1–N1, 2.294(2); Y1–N2, 2.345(2); Y1–N3, 2.319(2); Y1–O1, 2.344(2); Y1–O2, 2.358(2); Y1–H3s, 2.30(3); Si3–H3s, 1.52(2). Selected interatomic angles (deg): N1–Y1–N2, 117.59(6); N2–Y1–N3, 125.42(6); N3–Y1–N1, 116.90(6); O1–Y1–O2, 157.61(6)°.

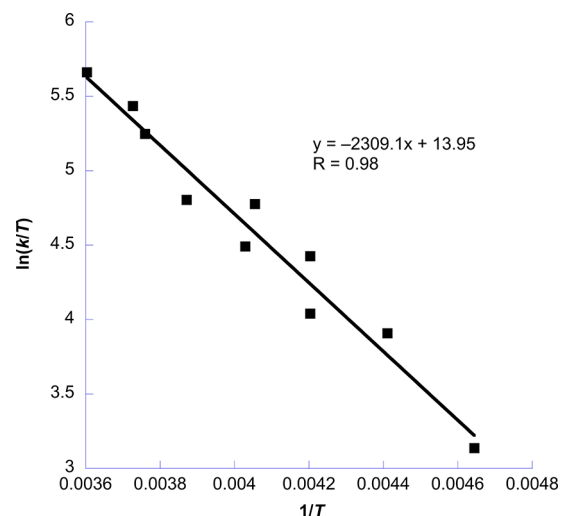
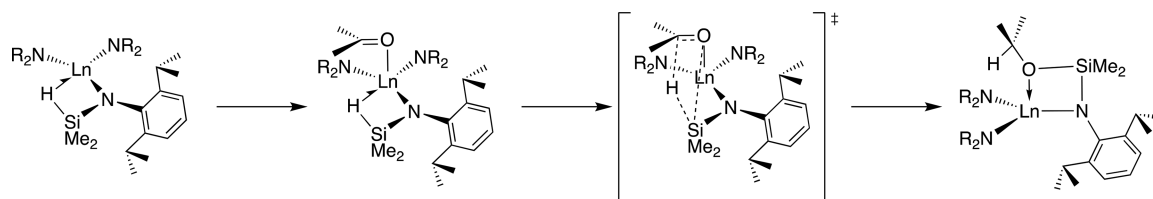


Figure 12. Eyring plot of exchange of **4c_{py}** and pyridine from integrated EXSY data.

correlations measured in $^1H-^{89}Y$ HSQC experiments, on the basis of through-bond J coupling, indicate that the yttrium–hydrogen bonding contains significant covalent character in $Ln\leftarrow H-Si$ structures.

THF coordination may be inhibited by the steric properties of bulky silazido ligands, but L-type oxygen donation does not necessarily block the formation of $Ln\leftarrow H-Si$. Thus, the two THF ligands in five-coordinate $Ln\{N(SiHMe_2)Ph\}THF_2$ and the two silyl ether donors in five-coordinate $Y\{N(SiMe_2OCHMe_2)dipp\}_2\{N(SiHMe_2)dipp\}$ should lead to equivalent 10-electron species. The latter compound retains

Scheme 1. Proposed Pathway for Hydrosilylation of Ketones in Reactions of 4c or 4c_{py}

a Y–H–Si interaction and reacts via hydrosilylation, whereas the former compound contains only classical SiH groups and their silazido ligands react as bases with enolizable ketones.

These compounds, interestingly, adopt low-symmetry structures in the solid state, as indicated by multiple bands assigned to silicon–hydrogen stretching modes in infrared spectra and by structures determined by single-crystal X-ray diffraction. Low-temperature solution-phase NMR data also indicate that three silazido ligands are inequivalent and that the compounds adopt low-symmetry structures at low temperature. These features extend to compounds containing bridging Ln–H–Si bonding, which feature three ^1H NMR signals, three $^1J_{\text{SiH}}$ values, and three ^{29}Si NMR signals. The largest silazido ligand, which gives the low-symmetry complexes, also has the greatest difference in size of the two substituents on nitrogen. These rare-earth silazido complexes react with ketones via hydrosilylation, rather than insertion into the Ln–N bond or formation of an enolate. The ketone insertion into SiH is proposed to occur through coordination of the carbonyl oxygen to the rare-earth center.

EXPERIMENTAL SECTION

General Considerations. All manipulations were performed under a dry argon atmosphere using standard Schlenk techniques or under a nitrogen atmosphere in a glovebox unless otherwise indicated. Water and oxygen were removed from benzene, pentane, and ether solvents using an IT PureSolv system. Benzene- d_6 , tetrahydrofuran- d_8 , and toluene- d_8 were heated to reflux over Na/K alloy and vacuum-transferred. $\text{ScCl}_3(\text{THF})_3$ was prepared by reaction of Sc_2O_3 with concentrated HCl followed by dehydration with SOCl_2 according to the literature.⁵⁴ YCl_3 and LuCl_3 were purchased from Strem Chemicals and used as received. Aniline, 2,6-dimethylaniline, and 2,6-diisopropylaniline (Sigma-Aldrich) and dimethylchlorosilane (Gelest) were distilled before use. $n\text{BuLi}$ (Sigma-Aldrich) was used as received. $\text{HN}(\text{SiHMe}_2)\text{dipp}$ (**1c**), $\text{LiN}(\text{SiHMe}_2)\text{dipp}$ (**2c**), $\text{Sc}\{\text{N}(\text{SiHMe}_2)\text{dipp}\}_3$ (**3c**, CCDC #1838231), $\text{Y}\{\text{N}(\text{SiHMe}_2)\text{dipp}\}_3$ (**4c**, CCDC #1838233), $\text{Lu}\{\text{N}(\text{SiHMe}_2)\text{dipp}\}_3$ (**5c**, CCDC #1838230), and $\text{Y}\{\kappa^2\text{-N}(\text{SiMe}_2\text{OCHPhMe})\text{dipp}\}\{\text{N}(\text{SiHMe}_2)\text{dipp}\}_2$ (**4d**, CCDC #1838232) were prepared by following a previous report.⁴² ^1H , $^{13}\text{C}\{^1\text{H}\}$, and $^{29}\text{Si}\{^1\text{H}\}$ HMBC NMR spectra were measured on a Bruker DRX-400 spectrometer or a Bruker Avance III-600 spectrometer. Infrared spectra were measured on a Bruker Vertex 80 instrument, using KBr pellets (transmission mode). Elemental analyses were performed using a PerkinElmer 2400 Series II CHN/S instrument. X-ray diffraction data were collected on a Bruker APEX II diffractometer.

$\text{LiN}(\text{SiHMe}_2)\text{Ph}$ (2a**).** First, $\text{HN}(\text{SiHMe}_2)\text{Ph}$ (**1a**) was prepared. A mixture of aniline (4.83 mL, 0.0530 mol) and pentane (300 mL) was cooled to 0°C , and $n\text{BuLi}$ (21.2 mL, 0.0530 mol) was added in a dropwise fashion. The reaction mixture was warmed to room temperature and stirred overnight. A pale yellow solid precipitated, which was isolated by filtration. The solid was dissolved in diethyl ether (500 mL), and the solution was cooled to 0°C . ClSiHMe_2 (5.89 mL, 0.0530 mol) was added slowly, and the reaction mixture was warmed to room temperature and stirred overnight. The solution was filtered to remove the salts, and the filtrate was concentrated *in vacuo*. The resulting red liquid was distilled under full vacuum (34°C) to

obtain a colorless solution. The solution was a mixture of the desired $\text{HN}(\text{SiHMe}_2)\text{Ph}$ (**1a**, 4.34 g, 0.0287 mol, 54.2%) and the disilylaniline $\text{N}(\text{SiHMe}_2)_2\text{Ph}$ in a 10.5:1 ratio. This mixture was used directly in the synthesis of $\text{LiN}(\text{SiHMe}_2)\text{Ph}$ described below. ^1H NMR (benzene- d_6 , 600 MHz, 25°C): δ 7.13 (t, 2 H, $^3J_{\text{HH}} = 7.6$ Hz, *m*- C_6H_5), 6.77 (t, 1 H, $^3J_{\text{HH}} = 7.8$ Hz, *p*- C_6H_5), 6.61 (d, 2 H, $^3J_{\text{HH}} = 8.4$ Hz, *o*- C_6H_5), 4.82 (v oct, 1 H, $^1J_{\text{SiH}} = 200.1$ Hz, SiHMe_2), 2.93 (s, 1 H, NH), 0.07 (d, 6 H, $^3J_{\text{HH}} = 3.2$ Hz, SiHMe_2). $^{13}\text{C}\{^1\text{H}\}$ NMR (benzene- d_6 , 150 MHz, 25°C): δ 147.84 (*ipso*- C_6H_5), 129.96 (*m*- C_6H_5), 118.79 (*p*- C_6H_5), 116.73 (*o*- C_6H_5), -1.92 (SiHMe_2). $^{15}\text{N}\{^1\text{H}\}$ NMR (benzene- d_6 , 60.8 MHz, 25°C): δ -320.8 (NH). $^{29}\text{Si}\{^1\text{H}\}$ NMR (benzene- d_6 , 119.3 MHz, 25°C): δ -14.2 (SiHMe_2). IR (KBr, cm^{-1}): 3471 w, 3383 m, 3212 w, 3074 w, 3040 m, 2962 m, 2902 w, 2129 s (SiH), 1923 w, 1602 s, 1499 s, 1422 s, 1294 s, 1253 s, 1177 m, 1154 w, 1077 m, 1029 m, 997 m, 904 s, 834 m, 802 w, 752 s, 718 w, 692 s, 650 w, 632 w. The mixture (2.00 g) of silylaniline $\text{HN}(\text{SiHMe}_2)\text{Ph}$ (1.77 g, 0.0117 mol) and disilylaniline was added to pentane (40 mL) and cooled to -78°C . $n\text{BuLi}$ (4.68 mL, 0.0117 mol) was added in a dropwise manner, and a white precipitate formed as the addition occurred. The reaction mixture was warmed to room temperature and stirred overnight. The precipitate was isolated by filtration followed by pentane washings (2×20 mL). The white residue was dried under reduced pressure for 2.5 h to give the desired product as a white solid (1.37 g, 0.00872 mol, 74.5%). ^1H NMR (THF- d_8 , 600 MHz, 25°C): δ 6.71 (t, 2 H, $^3J_{\text{HH}} = 7.7$ Hz, *m*- C_6H_5), 6.42 (d, 2 H, $^3J_{\text{HH}} = 8.3$ Hz, *o*- C_6H_5), 6.05 (t, 1 H, $^3J_{\text{HH}} = 8.3$ Hz, *p*- C_6H_5), 4.72 (d, br, 1 H, $^1J_{\text{SiH}} = 176.9$ Hz, SiHMe_2), 0.10 (s, br, 3 H, SiHMe_2), 0.08 (s, br, 3 H, SiHMe_2). $^{13}\text{C}\{^1\text{H}\}$ NMR (thf- d_8 , 150 MHz, 25°C): δ 163.64 (*ipso*- C_6H_5), 128.73 (*m*- C_6H_5), 122.31 (*o*- C_6H_5), 111.00 (*p*- C_6H_5), 1.26 (SiHMe_2). $^{15}\text{N}\{^1\text{H}\}$ NMR (thf- d_8 , 60.8 MHz, 25°C): δ -280.8 . $^{29}\text{Si}\{^1\text{H}\}$ NMR (THF- d_8 , 119.3 MHz, 25°C): δ -29.2 (SiHMe_2). $^7\text{Li}\{^1\text{H}\}$ NMR (THF- d_8 , MHz, 25°C): δ 0.51(s). IR (KBr, cm^{-1}): 3384 m, 3065 w, 3051 w, 3014 m, 2898 w, 2525 w, 2069 s (SiH), 1926 w, 1585 s, 1546 m, 1479 s, 1384 w, 1293 s, 1244 s, 1179 m, 1151 w, 1075 m, 1027 m, 993 m, 931 s, 904 s, 885 s, 826 s, 767 s, 753 s, 699 s, 634 w. Anal. Calcd for $\text{C}_8\text{H}_{12}\text{LiNSi}$: C, 61.12; H, 7.69; N, 8.91. Found: C, 61.06; H, 7.71; N, 8.71. Mp: $238\text{--}240^\circ\text{C}$.

$\text{LiN}(\text{SiHMe}_2)\text{dmp}$ (2b**).** First, $\text{HN}(\text{SiHMe}_2)\text{dmp}$ (**1b**) was prepared. A mixture of H_2Ndmp (9.20 mL, 0.0747 mol; *dmp* = 2,6-dimethylphenyl) and pentane (300 mL) was cooled to 0°C , and $n\text{BuLi}$ (30.0 mL, 0.0747 mol) was slowly added in a dropwise manner. The reaction mixture was warmed to room temperature and stirred for 3 h, forming a white precipitate. The solid was isolated by filtration. The precipitate was dissolved in diethyl ether (500 mL), and the resulting solution was cooled to 0°C . ClSiHMe_2 (8.40 mL, 0.0747 mol) was then added in a dropwise fashion. The reaction mixture was warmed to room temperature and stirred for 3 h. The solution was filtered, and the volatile materials were evaporated *in vacuo*. The resulting yellow liquid was distilled under dynamic vacuum at 56°C to give the product as a colorless liquid (10.7 g, 0.0597 mol, 79.9%). ^1H NMR (benzene- d_6 , 600 MHz, 25°C): δ 7.00 (d, 2 H, $^3J_{\text{HH}} = 7.6$ Hz, *m*- $\text{C}_6\text{Me}_2\text{H}_3$), 6.86 (t, 1 H, $^3J_{\text{HH}} = 7.5$ Hz, *p*- $\text{C}_6\text{Me}_2\text{H}_3$), 4.87 (v oct, 1 H, $^1J_{\text{SiH}} = 201.5$ Hz, SiHMe_2), 2.18 (s, 6 H, $\text{C}_6\text{Me}_2\text{H}_3$), 1.89 (s, 1 H, NH), 0.05 (d, 6 H, $^3J_{\text{HH}} = 3.1$ Hz, SiHMe_2). $^{13}\text{C}\{^1\text{H}\}$ NMR (benzene- d_6 , 150 MHz, 25°C): δ 143.66 (*ipso*- $\text{C}_6\text{Me}_2\text{H}_3$), 131.08 (*o*- $\text{C}_6\text{Me}_2\text{H}_3$), 129.20 (*m*- $\text{C}_6\text{Me}_2\text{H}_3$), 122.38 (*p*- $\text{C}_6\text{Me}_2\text{H}_3$), 19.98 ($\text{C}_6\text{Me}_2\text{H}_3$), -0.89 (SiHMe_2). $^{15}\text{N}\{^1\text{H}\}$ NMR (benzene- d_6 , 60.8 MHz, 25°C): δ -333.5 . $^{29}\text{Si}\{^1\text{H}\}$ NMR (benzene- d_6 , 119.3 MHz, 25°C): δ -10.4 . IR (KBr, cm^{-1}): 3485 w, 3379 m (NH), 3074 w, 3026

w, 2960 s, 2920 m, 2855 m, 2732 w, 2126 s (SiH), 1912 w, 1842 w, 1781 w, 1724 w, 1626 m, 1596 m, 1475 s, 1432 s, 1373 s, 1318 w, 1254 s, 1219 s, 1163 w, 1098 s, 1031 w, 988 w, 910 s, 833 s, 804 w, 734 s, 700 w, 662 m, 633 w. HN(SiHMe₂)dmp (2.00 g, 0.0112 mol) in pentane (40 mL) was cooled to -78°C , and *n*BuLi (4.47 mL, 0.0112 mol) was added in a dropwise fashion. The reaction mixture was warmed to room temperature and stirred overnight. The solvent was evaporated under vacuum for 2 h to give the product as a white solid (1.73 g, 0.00933 mol, 83.3%). ¹H NMR (benzene-*d*₆, 600 MHz, 25 $^{\circ}\text{C}$): δ 6.93 (d, 2 H, ³J_{HH} = 7.3 Hz, *m*-C₆Me₂H₃), 6.70 (br t, 1 H, *p*-C₆Me₂H₃), 5.10 (br s, 1 H, ¹J_{SiH} = 164.8 Hz, SiHMe₂), 1.98 (s, 6 H, C₆Me₂H₃), 0.16 (br d, 6 H, SiHMe₂). ¹³C{¹H} NMR (benzene-*d*₆, 150 MHz, 25 $^{\circ}\text{C}$): δ 154.01 (*ipso*-C₆Me₂H₃), 131.56 (*o*-C₆Me₂H₃), 129.96 (*m*-C₆Me₂H₃), 120.00 (*p*-C₆Me₂H₃), 21.13 (C₆Me₂H₃), 1.14 (SiHMe₂). ¹⁵N{¹H} NMR (benzene-*d*₆, 60.8 MHz, 25 $^{\circ}\text{C}$): δ -305.4. ²⁹Si{¹H} NMR (benzene-*d*₆, 119.3 MHz, 25 $^{\circ}\text{C}$): δ -21.3. ⁷Li{¹H} NMR (benzene-*d*₆, MHz, 25 $^{\circ}\text{C}$): δ 1.97 (s). IR (KBr, cm⁻¹): 3374 w (NH), 3059 w, 3010 w, 2955 s, 2898 s, 2843 m, 2731 w, 2704 w, 2122 w (SiH), 2056 m (SiH), 1981 s (SiH), 1839 w, 1782 w, 1712 w, 1661 w, 1590 s, 1469 s, 1417 s, 1377 s, 1251 s, 1219 s, 1161 w, 1097 s, 935 s, 889 s, 827 s, 787 s, 759 s, 661 m, 638 m. Anal. Calcd for C₁₀H₁₆LiNSi: C, 64.83; H, 8.71; N, 7.56. Found: C, 64.85; H, 8.42; N, 7.24. Mp: 86–88 $^{\circ}\text{C}$.

ScLi(SiHMe₂)Ph₃(THF)₂ (3a). A solid mixture of ScCl₃(THF)₃ (0.0779 g, 0.212 mmol) and LiN(SiHMe₂)Ph (0.100 g, 0.636 mmol) was cooled to -78°C . THF (7 mL) was cooled to -78°C in a separate vessel. The cold THF was added to the solid mixture, and the reaction mixture was allowed to stand at -78°C for 1 h. The reaction mixture was warmed to room temperature and stirred overnight. The solvent was removed *in vacuo*, and the residue was extracted with pentane (3 \times 5 mL). The pentane extracts were combined, and the solvent was evaporated to give the desired product as a white sticky solid (0.113 g, 0.177 mmol, 83.5%). ¹H NMR (benzene-*d*₆, 600 MHz, 25 $^{\circ}\text{C}$): δ 7.19 (t, 6 H, ³J_{HH} = 7.3 Hz, *m*-C₆H₅), 7.08 (d, 6 H, ³J_{HH} = 7.8 Hz, *o*-C₆H₅), 6.87 (t, 3 H, ³J_{HH} = 7.0 Hz, *p*-C₆H₅), 5.24 (br, 3 H, ¹J_{SiH} = 175.9 Hz, SiHMe₂), 3.39 (s, br, 4 H, OCH₂CH₂), 0.89 (s, br, 4 H, OCH₂CH₂), 0.28 (d, 18 H, ³J_{HH} = 3.1 Hz, SiHMe₂). ¹³C{¹H} NMR (benzene-*d*₆, 150 MHz, 25 $^{\circ}\text{C}$): δ 153.33 (*ipso*-C₆H₅), 129.71 (*m*-C₆H₅), 126.06 (*o*-C₆H₅), 121.20 (*p*-C₆H₅), 72.46 (OCH₂CH₂), 25.23 (OCH₂CH₂), 0.10 (SiHMe₂). ¹⁵N{¹H} NMR (benzene-*d*₆, 60.8 MHz, 25 $^{\circ}\text{C}$): δ -214.1. ²⁹Si{¹H} NMR (benzene-*d*₆, 119.3 MHz, 25 $^{\circ}\text{C}$): δ -21.9. IR (KBr, cm⁻¹): 3381 w, 3068 w, 2957 m, 2897 w, 2531 w, 2113 m (SiH), 2064 m (SiH), 1932 w, 1586 s, 1475 s, 1384 w, 1242 s, 1167 m, 1069 m, 999 m, 898 s, 832 s, 805 s, 753 s, 696 s. Anal. Calcd for C₂₈H₄₄N₃OScSi₃ (one THF is lost during combustion analysis): C, 59.22; H, 7.81; N, 7.40. Found: C, 58.90; H, 7.70; N, 7.08. Mp: 110–112 $^{\circ}\text{C}$.

Y{N(SiHMe₂)Ph₃(THF)₂ (4a). YCl₃ (0.120 g, 0.614 mmol) and LiN(SiHMe₂)Ph (0.290 g, 1.84 mmol) were cooled to -78°C . THF (7 mL) was cooled to -78°C in a separate vessel. The cold THF was added to the solid mixture. The reaction mixture was allowed to stand at -78°C for 1 h, and then it was warmed to room temperature and stirred overnight. The solvent was removed under reduced pressure, and the residue was extracted with pentane (3 \times 5 mL). The pentane extracts were combined, and the solvent was evaporated to give the desired product as a white sticky solid (0.0995 g, 0.145 mmol, 23.7%). ¹H NMR (benzene-*d*₆, 600 MHz, 25 $^{\circ}\text{C}$): δ 7.22 (t, 6 H, ³J_{HH} = 7.7 Hz, *m*-C₆H₅), 7.07 (d, 6 H, ³J_{HH} = 8.6 Hz, *o*-C₆H₅), 6.83 (t, 3 H, ³J_{HH} = 7.4 Hz, *p*-C₆H₅), 4.95 (sept, 3 H, ³J_{HH} = 3.1 Hz, ¹J_{SiH} = 173.2 Hz, SiHMe₂), 3.68 (s, 8 H, OCH₂CH₂), 1.11 (s, 8 H, OCH₂CH₂), 0.39 (d, 18 H, ³J_{HH} = 3.3 Hz, SiHMe₂). ¹³C{¹H} NMR (benzene-*d*₆, 150 MHz, 25 $^{\circ}\text{C}$): δ 155.33 (*ipso*-C₆H₅), 129.82 (*m*-C₆H₅), 124.89 (*o*-C₆H₅), 119.17 (*p*-C₆H₅), 71.53 (OCH₂CH₂), 25.48 (OCH₂CH₂), 0.59 (SiHMe₂). ¹⁵N{¹H} NMR (benzene-*d*₆, 60.8 MHz, 25 $^{\circ}\text{C}$): δ -235.0. ²⁹Si{¹H} NMR (benzene-*d*₆, 119.3 MHz, 25 $^{\circ}\text{C}$): δ -24.7 (SiHMe₂). IR (KBr, cm⁻¹): 3383 w, 3067 w, 3047 w, 2958 m, 2896 w, 2531 w, 2117 m (SiH), 2075 m (SiH), 1588 s, 1481 s, 1384 w, 1293 m, 1256 s, 1244 s, 1219 s, 1181 w, 1076 w, 1019 m, 995 m, 919 s, 876 s, 831 m, 791 m, 697 s, 646 w, 630 w. Anal. Calcd for

C₃₂H₅₂N₃O₂Si₃Y: C, 56.20; H, 7.66; N, 6.14. Found: C, 56.23; H, 7.67; N, 6.13. Mp: 114–116 $^{\circ}\text{C}$.

Lu{N(SiHMe₂)Ph₃(THF)₂ (5a). LuCl₃ (0.145 g, 0.515 mmol) and LiN(SiHMe₂)Ph (0.243 g, 1.54 mmol) were cooled to -78°C . THF (7 mL) was cooled to -78°C in a separate vessel. The cold THF was added to the solid mixture, and the reaction mixture was allowed to stand for 1 h at -78°C . The mixture was warmed to room temperature and stirred overnight. The solvent was removed under vacuum, and the residue was extracted with pentane (3 \times 5 mL). The pentane extracts were combined, and the solvent was evaporated to give the desired product as a white sticky solid (0.0984 g, 0.128 mmol, 24.8%). ¹H NMR (benzene-*d*₆, 600 MHz, 25 $^{\circ}\text{C}$): δ 7.22 (t, 6 H, ³J_{HH} = 7.5 Hz, *m*-C₆H₅), 7.12 (d, 6 H, ³J_{HH} = 7.5 Hz, *o*-C₆H₅), 6.83 (t, 3 H, ³J_{HH} = 7.1 Hz, *p*-C₆H₅), 4.90 (sept, 3 H, ³J_{HH} = 3.1 Hz, ¹J_{SiH} = 173.6 Hz, SiHMe₂), 3.66 (s, 8 H, OCH₂CH₂), 1.09 (s, 8 H, OCH₂CH₂), 0.40 (d, 18 H, ³J_{HH} = 3.2 Hz, SiHMe₂). ¹³C{¹H} NMR (benzene-*d*₆, 150 MHz, 25 $^{\circ}\text{C}$): δ 155.21 (*ipso*-C₆H₅), 129.76 (*m*-C₆H₅), 125.30 (*o*-C₆H₅), 119.47 (*p*-C₆H₅), 71.68 (OCH₂CH₂), 25.50 (OCH₂CH₂), 0.53 (SiHMe₂). ¹⁵N{¹H} NMR (benzene-*d*₆, 60.8 MHz, 25 $^{\circ}\text{C}$): δ -233.6. ²⁹Si{¹H} NMR (benzene-*d*₆, 119.3 MHz, 25 $^{\circ}\text{C}$): δ -23.0. IR (KBr, cm⁻¹): 3380 w, 3069 w, 3046 w, 2958 m, 2896 w, 2532 w, 2123 m (SiH), 2081 m (SiH), 1932 w, 1589 s, 1480 s, 1384 w, 1243 s, 1213 s, 1180 w, 1076 w, 1016 m, 995 m, 918 s, 884 s, 831 m, 793 m, 754 s, 698 s, 646 w, 630 w. Anal. Calcd for C₃₂H₅₂LuN₃O₂Si₃: C, 49.92; H, 6.81; N, 5.46. Found: C, 50.38; H, 6.67; N, 5.55. Mp: 118–120 $^{\circ}\text{C}$.

Y{N(SiHMe₂)dmp₃THF (4b). YCl₃ (0.104 g, 0.531 mmol) and LiN(SiHMe₂)dmp (0.295 g, 1.59 mmol) were cooled to -78°C . THF (7 mL) was cooled to -78°C separately and added to the solid mixture. The reaction mixture was stirred at -78°C for 1 h, warmed to room temperature, and stirred overnight. The solvent was evaporated under vacuum, and the solid was extracted with pentane (3 \times 5 mL). The pentane extract was dried under vacuum to give the product as a sticky solid (0.265 g, 0.381 mmol, 71.7%). ¹H NMR (benzene-*d*₆, 600 MHz, 25 $^{\circ}\text{C}$): δ 7.10 (d, 6 H, ³J_{HH} = 7.4 Hz, *m*-C₆Me₂H₃), 6.84 (t, 3 H, ³J_{HH} = 7.4 Hz, *p*-C₆Me₂H₃), 5.20 (s, broad, 3 H, ¹J_{SiH} = 151.3 Hz, SiHMe₂), 3.45 (s, broad, 4 H, OCH₂CH₂), 2.36 (s, 18 H, C₆Me₂H₃), 0.94 (s, broad, 4 H, OCH₂CH₂), 0.15 (broad, 18 H, SiHMe₂). ¹³C{¹H} NMR (benzene-*d*₆, 150 MHz, 25 $^{\circ}\text{C}$): δ 151.02 (*ipso*-C₆Me₂H₃), 132.86 (*o*-C₆Me₂H₃), 129.01 (*m*-C₆Me₂H₃), 120.95 (*p*-C₆Me₂H₃), 72.24 (OCH₂CH₂), 25.06 (OCH₂CH₂), 21.72 (C₆Me₂H₃), 2.19 (SiHMe₂). ¹⁵N{¹H} NMR (benzene-*d*₆, 60.8 MHz, 25 $^{\circ}\text{C}$): δ -234.6. ²⁹Si{¹H} NMR (benzene-*d*₆, 119.3 MHz, 25 $^{\circ}\text{C}$): δ -25.3. IR (KBr, cm⁻¹): 3059 w, 2948 m, 2095 m, 2057 m (SiH), 1966 w (SiH), 1590 m, 1468 s, 1420 s, 1370 w, 1252 s, 1218 s, 1098 m, 1006 m, 927 s, 882 s, 834 s, 796 s, 762 s, 661 w, 635 w. Anal. Calcd for C₃₄H₅₆N₃OSi₃Y: C, 58.67; H, 8.11; N, 6.04. Found: C, 58.52; H, 8.19; N, 5.97. Mp: 142–144 $^{\circ}\text{C}$.

Lu{N(SiHMe₂)dmp₃THF (5b). LuCl₃ (0.468 g, 1.66 mmol) and LiN(SiHMe₂)dmp (0.924 g, 4.99 mmol) were cooled to -78°C . THF (7 mL) was cooled to -78°C separately and added to the solid mixture. The reaction mixture was stirred at -78°C for 1 h, warmed to room temperature, and stirred overnight. The solvent was evaporated under vacuum, and the solid was extracted with benzene (3 \times 5 mL). The benzene extract was dried under vacuum to give the product as a white solid (1.02 g, 1.31 mmol, 78.6%). ¹H NMR (benzene-*d*₆, 600 MHz, 25 $^{\circ}\text{C}$): δ 7.11 (d, 6 H, ³J_{HH} = 7.3 Hz, *m*-C₆Me₂H₃), 6.85 (t, 3 H, ³J_{HH} = 7.4 Hz, *p*-C₆Me₂H₃), 5.20 (sept, 3 H, ¹J_{SiH} = 155.8 Hz, SiHMe₂), 3.57 (s, broad, 4 H, OCH₂CH₂), 3.56 (s, broad, 8 H, residual THF), 2.39 (s, 18 H, C₆Me₂H₃), 1.41 (s, broad, 8 H, residual THF), 0.97 (s, broad, 4 H, OCH₂CH₂), 0.13 (d, 18 H, ³J_{HH} = 3.0 Hz, SiHMe₂). ¹³C{¹H} NMR (benzene-*d*₆, 150 MHz, 25 $^{\circ}\text{C}$): δ 151.17 (*ipso*-C₆Me₂H₃), 133.53 (*o*-C₆Me₂H₃), 128.99 (*m*-C₆Me₂H₃), 121.23 (*p*-C₆Me₂H₃), 73.06 (OCH₂CH₂), 68.28 (residual THF), 26.08 (residual THF), 25.10 (OCH₂CH₂), 21.77 (C₆Me₂H₃), 2.00 (SiHMe₂). ¹⁵N{¹H} NMR (benzene-*d*₆, 60.8 MHz, 25 $^{\circ}\text{C}$): δ -235.2. ²⁹Si{¹H} NMR (benzene-*d*₆, 119.3 MHz, 25 $^{\circ}\text{C}$): δ -23.7. IR (KBr, cm⁻¹): 3057 m, 3031 m, 2970 s, 2945 s, 2886 s, 2071 s (SiH), 1902 w (SiH), 1832 w, 1764 w, 1589 s, 1464 s, 1417 s, 1370 m, 1254 s, 1216 s, 1098 s, 1045 s, 936 s, 873 s, 831 s, 798 s, 758 s, 733 s, 674

m, 659 m, 634 m. Anal. Calcd for $C_{34}H_{56}LuN_3OSi_3$: C, 52.22; H, 7.22; N, 5.37. Found: C, 52.49; H, 7.38; N, 5.09. Mp: 130–132 °C.

Y{N(SiHMe₂)dipp}₃NC₅H₅ (4c-py). Y{N(SiHMe₂)dipp}₃ (0.142 g, 0.179 mmol) was dissolved in benzene (3 mL), and pyridine (0.0144 mL, 0.179 mmol) was added to the solution. The reaction mixture was stirred for 10 min, and the solvent was evaporated under reduced pressure. The resulting oily residue was extracted with pentane (3 × 5 mL) and the extract was concentrated and cooled to –30 °C to provide the desired product as a white crystalline solid (0.0893 g, 0.102 mmol, 57.2%). ¹H NMR (benzene-*d*₆, 600 MHz, 25 °C): δ 8.07 (br s, 2 H, *o*-NC₅H₅), 7.15 (br s, 6 H, *m*-C₆H₅), 7.05 (t, 3 H, ³J_{HH} = 7.3 Hz, *p*-C₆H₅), 6.60 (br s, 1 H, *p*-NC₅H₅), 6.35 (br s, 2 H, *m*-NC₅H₅), 5.33 (br s, 3 H, ¹J_{SiH} = 150.5 Hz, SiHMe₂), 3.64 (br s, 6 H, CHMe₂), 1.24 (br s, 18 H, CHMe₂), 1.00 (br s, 18 H, CHMe₂), 0.21 (br s, 18 H, SiHMe₂). ¹³C{¹H} NMR (benzene-*d*₆, 150 MHz, 25 °C): δ 149.51 (*o*-NC₅H₅), 148.78 (*ipso*-C₆H₅), 143.50 (*o*-C₆H₅), 140.24 (*p*-NC₅H₅), 124.89 (*m*-NC₅H₅), 124.53 (*m*-C₆H₅), 121.91 (*p*-C₆H₅), 27.92 (CHMe₂), 26.84 (CHMe₂), 25.67 (CHMe₂), 2.45 (SiHMe₂). ²⁹Si{¹H} NMR (benzene-*d*₆, 119.3 MHz, 25 °C): δ –26.54. IR (KBr, cm^{–1}): 3067 w, 3049 w, 2963 s, 2869 m, 2103 m (SiH), 1959 w (SiH), 1623 w, 1604 m, 1588 w, 1462 s, 1444 m, 1425 s, 1383 w, 1361 w, 1309 m, 1259 s, 1188 s, 1156 w, 1144 w, 1107 s, 1055 s, 1040 s, 1011 s, 933 s, 912 s, 864 w, 786 s, 756 s, 704 m, 675 w, 631 w. Anal. Calcd for C₄₇H₇₇N₄Si₃Y: C, 64.79; H, 8.91; N, 6.43. Found: C, 64.66; H, 8.83; N, 6.43. Mp: 156–158 °C.

Lu{N(SiMe₂OCHMePh)dipp}{N(SiHMe₂)dipp}₂ (5d). Lu{N(SiHMe₂)dipp}₃ (0.1781 g, 0.203 mmol) was dissolved in benzene (3 mL), and acetophenone (23.6 μL, 0.203 mmol) was added to the solution. The reaction mixture was stirred for 15 min, and the solvent was evaporated under reduced pressure. The resulting oily residue was extracted with pentane (3 × 5 mL), and the extract was concentrated and cooled to –30 °C to provide the desired product as a white crystalline solid (0.133 g, 0.125 mmol, 61.4%). ¹H NMR (benzene-*d*₆, 600 MHz, 25 °C): δ 7.19–6.95 (14 H, aromatic region), 5.57 (br s, 2 H, ¹J_{SiH} = 135.3 Hz, SiHMe₂), 5.06 (q, 1 H, ³J_{HH} = 6.5 Hz, OCHMePh), 3.85 (br vt, 4 H, CHMe₂), 3.66 (v pentet, 2 H, ³J_{HH} = 5.7 Hz, CHMe₂), 1.39 (d, 3 H, ³J_{HH} = 6.5 Hz, OCHMePh), 1.32 (br, 12 H, CHMe₂), 1.26 (br, 12 H, CHMe₂), 1.19 (d, 6 H, ³J_{HH} = 6.6 Hz, CHMe₂), 1.00 (br s, 6 H, CHMe₂), 0.40 (br s, 12 H, SiHMe₂), 0.21 (s, 3 H, SiMe₂), –0.24 (s, 3 H, SiMe₂). ¹³C{¹H} NMR (benzene-*d*₆, 150 MHz, 25 °C): δ 148.25, 145.07, 144.60, 143.62, 143.42, 141.81, 129.40, 129.30, 128.68, 127.22, 124.83, 124.28, 122.46, 122.35 (aromatic region), 78.09 (OCHMePh), 27.95 (CHMe₂), 27.71 (CHMe₂), 27.30 (CHMe₂), 27.09 (CHMe₂), 26.48 (OCHMePh), 26.19 (CHMe₂), 24.23 (CHMe₂), 4.23 (SiMe₂), 3.91 (SiHMe₂), 2.57 (SiMe₂). ²⁹Si{¹H} NMR (benzene-*d*₆, 119.3 MHz, 40 °C): δ 3.46 (SiMe₂). IR (KBr, cm^{–1}): 3388 w, 3051 w, 2962 s, 2929 m, 2868 m, 2109 w (SiH, from hydrolysis), 2001 w (SiH), 1881 m (SiH), 1621 w, 1588 w, 1494 w, 1460 s, 1427 s, 1382 w, 1361 w, 1307 m, 1251 s, 1238 s, 1190 s, 1148 w, 1110 s, 1060 m, 1038 s, 1009 w, 996 w, 951 m, 922 s, 910 s, 859 m, 838 s, 812 m, 781 s, 763 m, 748 m, 702 m, 676 w, 637 w, 606 w. Anal. Calcd for C₅₅H₉₂N₃O₃Si₃Lu (includes C₅H₁₂): C, 61.76; H, 8.66; N, 3.93. Found: C, 61.85; H, 8.65; N, 3.75. Mp: 184–186 °C.

Y{N(SiMe₂OCHPh₂)dipp}{N(SiHMe₂)dipp}₂ (4e). Y{N(SiHMe₂)dipp}₃ (0.0614 g, 0.0775 mmol) was dissolved in benzene (3 mL), and benzophenone (0.0141 g, 0.0775 mmol) was added to the solution. The reaction mixture was stirred for 15 min, and the solvent was evaporated under reduced pressure. The resulting oily residue was extracted with pentane (3 × 5 mL), and the extract was concentrated and cooled to –30 °C to provide the desired product as a white crystalline solid (0.0426 g, 0.0437 mmol, 56.4%). ¹H NMR (benzene-*d*₆, 600 MHz, 25 °C): δ 7.29–6.88 (19 H, aromatic region), 6.53 (s, 1 H, OCHPh₂), 5.01 (br s, 2 H, ¹J_{SiH} = 131.9 Hz, SiHMe₂), 3.71 (v pentet, 2 H, ³J_{HH} = 6.5 Hz, CHMe₂), 3.65 (br, 4 H, CHMe₂), 1.26 (br, 24 H, CHMe₂), 1.13 (br, 12 H, CHMe₂), 0.21 (br s, 12 H, SiHMe₂), 0.05 (s, 6 H, SiMe₂). ¹³C{¹H} NMR (benzene-*d*₆, 150 MHz, 25 °C): δ 148.59, 146.13, 144.30, 142.60, 140.94, 129.64, 129.30, 124.85, 124.42, 122.31, 121.87 (aromatic region), 83.42 (OCHPh₂), 28.19(CHMe₂), 27.94 (CHMe₂), 26.68 (CHMe₂), 26.56 (CHMe₂),

4.33 (SiMe₂), 3.10 (SiHMe₂). ²⁹Si{¹H} NMR (benzene-*d*₆, 119.3 MHz, 40 °C): δ –24.1 (SiHMe₂), 4.84 (SiMe₂). IR (KBr, cm^{–1}): 3387 w, 3062 w, 2962 s, 2929 s, 2869 m, 2108 w (SiH, from hydrolysis), 1965 w (SiH), 1886 w (SiH), 1620 w, 1588 w, 1459 s, 1425 s, 1382 w, 1360 w, 1306 s, 1251 s, 1235 s, 1187 s, 1148 w, 1110 m, 1056 m, 1040 m, 998 s, 933 s, 914 s, 861 m, 837 s, 814 m, 782 s, 745 s, 702 s, 678 w, 632 w. Anal. Calcd for C₅₅H₈₂N₃O₃Si₃Y: C, 67.79; H, 8.48; N, 4.31. Found: C, 68.24; H, 7.94; N, 3.95. Mp: 187–189 °C.

Lu{N(SiMe₂OCHPh₂)dipp}{N(SiHMe₂)dipp}₂ (5e). Lu{N(SiHMe₂)dipp}₃ (0.0533 g, 0.0607 mmol) was dissolved in benzene (3 mL), and benzophenone (0.0110 g, 0.0609 mmol) was added to the solution. The reaction mixture was stirred for 15 min, and the solvent was evaporated under reduced pressure. The resulting oily residue was extracted with pentane (3 × 5 mL), and the extract was concentrated and cooled to –30 °C to provide the desired product as a white crystalline solid (0.0375 g, 0.0352 mmol, 58.0%). ¹H NMR (benzene-*d*₆, 600 MHz, 25 °C): δ 7.24–6.87 (19 H, aromatic region), 6.62 (s, 1 H, OCHPh₂), 5.29 (br s, 2 H, ¹J_{SiH} = 133.1 Hz, SiHMe₂), 3.72 (br s, 6 H, CHMe₂), 1.26 (br, 24 H, CHMe₂), 1.12 (br, 12 H, CHMe₂), 0.26 (br s, 12 H, SiHMe₂), 0.05 (s, 6 H, SiMe₂). ¹³C{¹H} NMR (benzene-*d*₆, 150 MHz, 25 °C): δ 148.69, 146.15, 144.94, 143.15, 141.11, 129.41, 129.14, 124.95, 124.31, 122.54, 122.09 (aromatic region), 83.58 (OCHPh₂), 28.24(CHMe₂), 27.79 (CHMe₂), 26.80 (CHMe₂), 26.65 (CHMe₂), 4.49 (SiMe₂), 3.12 (SiHMe₂). ²⁹Si{¹H} NMR (benzene-*d*₆, 119.3 MHz, 40 °C): δ –21.79 (SiHMe₂), –4.10 (SiMe₂). IR (KBr, cm^{–1}): 3387 w, 3059 w, 3046 w, 3008 s, 2963 s, 2869 m, 2110 w (SiH, from hydrolysis), 1957 m (SiH), 1619 w, 1587 w, 1497 w, 1458 s, 1425 s, 1382 m, 1360 w, 1317 m, 1305 s, 1248 s, 1235 s, 1188 s, 1147 w, 1098 m, 1059 m, 1040 m, 994 s, 935 s, 910 s, 875 m, 834 s, 804 m, 781 s, 749 m, 738 m, 702 s, 681 w, 655 w, 628 w. Anal. Calcd for C₅₅H₈₂N₃O₃Si₃Lu: C, 62.29; H, 7.79; N, 3.96. Found: C, 62.35; H, 8.16; N, 3.85. Mp: 190–192 °C.

Y{N(SiMe₂OCHMe₂)dipp}₂{N(SiHMe₂)dipp} (4f). Y{N(SiHMe₂)dipp}₃ (0.105 g, 0.132 mmol) was dissolved in toluene (3 mL) and cooled to –78 °C. Acetone (0.0215 mL, 0.291 mmol) was added to the cold solution, and the reaction mixture was stirred for 10 min. The solvent was evaporated under vacuum. The resulting oily residue was washed with pentane (3 × 5 mL) and dried under reduced pressure to provide the desired product as a white solid (0.0678 g, 0.0746 mmol, 56.3%). Recrystallization from pentane at –30 °C provided X-ray-quality crystals. ¹H NMR (benzene-*d*₆, 600 MHz, 25 °C): δ 7.24–7.03 (9 H, aromatic region), 5.57 (br s, 1 H, ¹J_{SiH} = 138.7 Hz, SiHMe₂), 4.17 (v pent, 2 H, ³J_{HH} = 6.5 Hz, OCHMe₂), 3.98 (v pent, 2 H, ³J_{HH} = 6.5 Hz, CHMe₂), 3.71 (br, 3 H, CHMe₂), 3.54 (v triplet, 1 H, ³J_{HH} = 6.5 Hz, CHMe₂), 1.52 (br d, 6 H, ³J_{HH} = 7 Hz, CHMe₂), 1.48 (d, 3 H, ³J_{HH} = 6.6 Hz, CHMe₂), 1.42 (d, 6 H, ³J_{HH} = 6.6 Hz, CHMe₂), 1.29 (v triplet, 6 H, ³J_{HH} = 5.5 Hz, CHMe₂), 1.23 (d, 6 H, ³J_{HH} = 6.4 Hz, CHMe₂), 1.19 (d, 3 H, ³J_{HH} = 6.7 Hz, CHMe₂), 0.93 (br s, 6 H, CHMe₂), 0.88 (d, 6 H, ³J_{HH} = 6.1 Hz, OCHMe₂), 0.84 (d, 6 H, ³J_{HH} = 6.1 Hz, OCHMe₂), 0.49 (d, 3 H, ³J_{HH} = 2.2 Hz, SiHMe₂), 0.34 (d, 3 H, ³J_{HH} = 2.4 Hz, SiHMe₂), 0.32 (s, 6 H, SiMe₂), 0.23 (s, 6 H, SiMe₂). ¹³C{¹H} NMR (benzene-*d*₆, 150 MHz, 25 °C): δ 150.03 (*ipso*-dipp), 147.24 (*ipso*-dipp), 144.36 (CCHMe₂), 144.09 (CCHMe₂), 143.55 (CCHMe₂), 143.12 (CCHMe₂), 124.85 (*m*-dipp), 124.72 (*m*-dipp), 124.60 (*m*-dipp), 123.91 (*m*-dipp), 123.80 (*p*-dipp), 121.79 (*p*-dipp), 71.33 (OCHMe₂), 28.38 (CHMe₂), 28.28 (CHMe₂), 28.09 (CHMe₂), 27.95 (CHMe₂), 27.40 (CHMe₂), 27.35 (CHMe₂), 27.29 (CHMe₂), 26.87 (CHMe₂), 26.70 (CHMe₂), 26.37 (CHMe₂), 25.59 (OCHMe₂), 24.91(OCHMe₂), 5.21 (SiHMe₂), 4.99 (SiMe₂), 4.12 (SiMe₂), 3.55 (SiHMe₂). ²⁹Si{¹H} NMR (benzene-*d*₆, 119.3 MHz, 40 °C): δ –25.4 (SiHMe₂), 0.23 (SiMe₂). IR (KBr, cm^{–1}): 3050 w, 2964 s, 2870 m, 1991 w (SiH), 1622 w, 1588 w, 1462 s, 1423 s, 1381 m, 1361 w, 1306 s, 1251 s, 1229 s, 1181 s, 1143 w, 1109 s, 1039 w, 960 s, 937 s, 873 w, 859 w, 836 s, 812 m, 779 s, 745 w, 701 w, 680 w, 629 w. Anal. Calcd for C₄₈H₈₄N₃O₂Si₃Y: C, 63.47; H, 9.32; N, 4.63. Found: C, 63.02; H, 9.34; N, 4.50. Mp: 215–217 °C.

■ ASSOCIATED CONTENT

■ Supporting Information

The Supporting Information is available free of charge at <https://pubs.acs.org/doi/10.1021/acs.organomet.1c00162>.

NMR and IR spectra of the compounds HN(SiHMe₂)-Ph (1a), HN(SiHMe₂)dmp (1b), LiN(SiHMe₂)Ph (2a), LiN(SiHMe₂)dmp (2b), Sc{N(SiHMe₂)-Ph}₃(THF)₂ (3a), Y{N(SiHMe₂)Ph}₃(THF)₂ (4a), Lu{N(SiHMe₂)Ph}₃(THF)₂ (5a), Y{N(SiHMe₂)dmp}₃(THF) (4b), Lu{N(SiHMe₂)dmp}₃(THF) (5b), Y{N(SiHMe₂)dipp}₃NC₅H₅ (4c·py), Lu{N(SiMe₂OCHMePh)dipp}₂{N(SiHMe₂)dipp}₂ (5d), Y{N(SiMe₂OCHPh₂)dipp}₂{N(SiHMe₂)dipp}₂ (4e), Lu{N(SiMe₂OCHPh₂)dipp}₂{N(SiHMe₂)dipp}₂ (5e), and Y{N(SiMe₂OCHMe₂)dipp}₂{N(SiHMe₂)dipp} (4f) (PDF)

Accession Codes

CCDC 2068522–2068531 contain the supplementary crystallographic data for this paper. These data can be obtained free of charge via www.ccdc.cam.ac.uk/data_request/cif, or by emailing data_request@ccdc.cam.ac.uk, or by contacting The Cambridge Crystallographic Data Centre, 12 Union Road, Cambridge CB2 1EZ, UK; fax: +44 1223 336033.

■ AUTHOR INFORMATION

Corresponding Author

Aaron D. Sadow – US Department of Energy Ames Laboratory and Department of Chemistry, Iowa State University, Ames, Iowa 50011, United States; orcid.org/0000-0002-9517-1704; Email: sadow@iastate.edu

Authors

Kasuni C. Boteju – US Department of Energy Ames Laboratory and Department of Chemistry, Iowa State University, Ames, Iowa 50011, United States

Amrit Venkatesh – US Department of Energy Ames Laboratory and Department of Chemistry, Iowa State University, Ames, Iowa 50011, United States; orcid.org/0000-0001-5319-9269

Yang-Yun Chu – Department of Chemistry, Iowa State University, Ames, Iowa 50011, United States

Suchen Wan – US Department of Energy Ames Laboratory, Iowa State University, Ames, Iowa 50011, United States

Arkady Ellern – Department of Chemistry, Iowa State University, Ames, Iowa 50011, United States

Aaron J. Rossini – US Department of Energy Ames Laboratory and Department of Chemistry, Iowa State University, Ames, Iowa 50011, United States; orcid.org/0000-0002-1679-9203

Complete contact information is available at: <https://pubs.acs.org/doi/10.1021/acs.organomet.1c00162>

Notes

The authors declare no competing financial interest.

■ ACKNOWLEDGMENTS

This research was supported by the U.S. Department of Energy (DOE), Office of Science, Basic Energy Sciences, Division of Chemical Sciences, Geosciences, and Biosciences (K.C.B., S.W., and A.D.S., synthesis and reactivity). Ames Laboratory is operated for the DOE by Iowa State University under Contract No. DE-AC02-07CH11358. A.V. and A.J.R. acknowledge

support from the donors of the American Chemical Society Petroleum Research Fund (58627-DNI6; 2D NMR experiments).

■ REFERENCES

- (1) Anwander, R., Lanthanide amides. In *Organolanthanoid Chemistry: Synthesis, Structure, Catalysis*; Springer Berlin Heidelberg: 1996; pp 33–112.
- (2) Schumann, H. Homoleptic Organometallic Compounds of the Rare Earths. *Comments Inorg. Chem.* **1983**, *2*, 247–259.
- (3) Zimmermann, M.; Anwander, R. Homoleptic Rare-Earth Metal Complexes Containing Ln–C σ -Bonds. *Chem. Rev.* **2010**, *110*, 6194–6259.
- (4) Harder, S. Syntheses and Structures of Homoleptic Lanthanide Complexes with Chelating *o*-Dimethylaminobenzyl Ligands: Key Precursors in Lanthanide Chemistry. *Organometallics* **2005**, *24*, 373–379.
- (5) Behrle, A. C.; Schmidt, J. A. R. Synthesis and Reactivity of Homoleptic α -Metalated *N,N*-Dimethylbenzylamine Rare-Earth-Metal Complexes. *Organometallics* **2011**, *30*, 3915–3918.
- (6) Schumann, H. Synthesis, Structure and Reactivity of Homoleptic Organolanthanoids. *J. Less-Common Met.* **1985**, *112*, 327–341.
- (7) Kawaoka, A. M.; Douglass, M. R.; Marks, T. J. Homoleptic Lanthanide Alkyl and Amide Precatalysts Efficiently Mediate Intramolecular Hydrophosphination/cyclization. Observations on Scope and Mechanism. *Organometallics* **2003**, *22*, 4630–4632.
- (8) Zimmermann, M.; Frøystein, N. Å.; Fischbach, A.; Sirsch, P.; Dietrich, H. M.; Törnroos, K. W.; Herdtweck, E.; Anwander, R. Homoleptic Rare-Earth Metal(III) Tetramethylaluminates: Structural Chemistry, Reactivity, and Performance in Isoprene Polymerization. *Chem. - Eur. J.* **2007**, *13*, 8784–8800.
- (9) Roesky, P. W.; Gamer, M. T.; Puchner, M.; Greiner, A. Homoleptic Lanthanide Complexes of Chelating Bis(phosphanyl)-amides: Synthesis, Structure, and Ring-Opening Polymerization of Lactones. *Chem. - Eur. J.* **2002**, *8*, 5265–5271.
- (10) Burgstein, M. R.; Berberich, H.; Roesky, P. W. Homoleptic Lanthanide Amides as Homogeneous Catalysts for Alkyne Hydroamination and the Tishchenko Reaction. *Chem. - Eur. J.* **2001**, *7*, 3078–3085.
- (11) Woodruff, D. N.; Wimpenny, R. E. P.; Layfield, R. A. Lanthanide Single-Molecule Magnets. *Chem. Rev.* **2013**, *113*, 5110–5148.
- (12) Layfield, R. A. Organometallic Single-Molecule Magnets. *Organometallics* **2014**, *33*, 1084–1099.
- (13) Bradley, D. C.; Ghotra, J. S.; Hart, F. A. Three-co-ordination in Lanthanide Chemistry: Tris[bis(trimethylsilyl)amido]lanthanide(III) Compounds. *J. Chem. Soc., Chem. Commun.* **1972**, 349–350.
- (14) Andersen, R. A.; Templeton, D. H.; Zalkin, A. Structure of Tris(bis(trimethylsilyl)amido)neodymium(III), Nd[N(Si(CH₃)₃)₂]₃. *Inorg. Chem.* **1978**, *17*, 2317–2319.
- (15) Rees, W. S., Jr.; Just, O.; Van Derveer, D. S. Molecular Design of Dopant Precursors for Atomic Layer Epitaxy of SrS:Ce. *J. Mater. Chem.* **1999**, *9*, 249–252.
- (16) Herrmann, W. A.; Anwander, R.; Munck, F. C.; Scherer, W.; Dufaud, V.; Huber, N. W.; Artus, G. R. J. Lanthanoid Complexes. IX. Reactivity Control of Lanthanoid Amides Through Ligand Effects. Synthesis and Structures of Sterically Congested Alkoxy Complexes. *Z. Naturforsch., B: J. Chem. Sci.* **1994**, *49*, 1789–1797.
- (17) Ghotra, J. S.; Hursthouse, M. B.; Welch, A. J. Three Coordinate Scandium(III) and Europium(III); Crystal and Molecular Structures of Their Tris(hexamethyldisilylamides). *J. Chem. Soc., Chem. Commun.* **1973**, 669–670.
- (18) Mainz, V. V.; Andersen, R. A. Preparation and Stereochemistry of Bis(carboxylato)bis(tertiary phosphine)bis(disilylamido)-dimolybdenum(II) Complexes. *Inorg. Chem.* **1980**, *19*, 2165–2169.
- (19) Goodwin, C. A. P.; Joslin, K. C.; Lockyer, S. J.; Formanuk, A.; Morris, G. A.; Ortu, F.; Vitorica-Yrezabal, I. J.; Mills, D. P. Homoleptic Trigonal Planar Lanthanide Complexes Stabilized by

Superbulky Silylamide Ligands. *Organometallics* **2015**, *34*, 2314–2325.

(20) Gauvin, R. M.; Delevoye, L.; Hassan, R. A.; Keldenich, J.; Mortreux, A. Well-Defined Silica-Supported Rare-Earth Silylamides. *Inorg. Chem.* **2007**, *46*, 1062–1070.

(21) Fjeldberg, T.; Andersen, R. A. The Molecular Structure of Gaseous Tris(bis(trimethylsilyl)amido)scandium, $\text{Sc}\{\text{N}(\text{Si}(\text{CH}_3)_2)_2\}_3$, as Determined by Electron Diffraction: A Three-coordinate Scandium(III) Amide. *J. Mol. Struct.* **1985**, *128*, 49–57.

(22) Tilley, T. D.; Andersen, R. A.; Zalkin, A. Divalent Lanthanide Chemistry. Preparation and Crystal Structures of Sodium Tris[bis(trimethylsilyl)amido]europate(II) and Sodium Tris[bis(trimethylsilyl)amido]ytterbate(II), $\text{NaM}[\text{N}(\text{SiMe}_3)_2]_3$. *Inorg. Chem.* **1984**, *23*, 2271–2276.

(23) Niemeyer, M. Reactions of Hypersilyl Potassium with Rare-Earth Metal Bis(trimethylsilylamides): Addition versus Peripheral Deprotonation. *Inorg. Chem.* **2006**, *45*, 9085–9095.

(24) Anwender, R.; Roesky, R. Grafting of Versatile Lanthanide Silylamide Precursors Onto Mesoporous MCM-41. *J. Chem. Soc., Dalton Trans.* **1997**, 137–138.

(25) Liang, Y.; Anwender, R. Nanostructured Catalysts Via Metal Amide-promoted Smart Grafting. *Dalton Trans.* **2013**, *42*, 12521–12545.

(26) Hitchcock, P. B.; Lappert, M. F.; Smith, R. G.; Bartlett, R. A.; Power, P. P. Synthesis and Structural Characterization of the First Neutral Homoleptic Lanthanide Metal(III) Alkyls, $[\text{LnR}_3]$ [$\text{Ln} = \text{La}$ or Sm , $\text{R} = \text{CH}(\text{SiMe}_3)_2$]. *J. Chem. Soc., Chem. Commun.* **1988**, 1007–1009.

(27) Perrin, L.; Maron, L.; Eisenstein, O.; Lappert, M. F. Gamma Agostic C-H or Beta Agostic Si-C Bonds in $\text{La}\{\text{CH}(\text{SiMe}_3)_2\}_3$? A DFT Study of the Role of the Ligand. *New J. Chem.* **2003**, *27*, 121–127.

(28) Conley, M. P.; Lapadula, G.; Sanders, K.; Gajan, D.; Lesage, A.; del Rosal, I.; Maron, L.; Lukens, W. W.; Copéret, C.; Andersen, R. A. The Nature of Secondary Interactions at Electrophilic Metal Sites of Molecular and Silica-Supported Organolanthanum Complexes from Solid-State NMR Spectroscopy. *J. Am. Chem. Soc.* **2016**, *138*, 3831–3843.

(29) Avent, A. G.; Caro, C. F.; Hitchcock, P. B.; Lappert, M. F.; Li, Z. N.; Wei, X. H. Synthetic and Structural Experiments on Yttrium, Cerium and Magnesium Trimethylsilylmethyls and Their Reaction Products with Nitriles; with a Note on Two Cerium Gamma-diketiminates. *J. Chem. Soc., Dalton Trans.* **2004**, 1567–1577.

(30) Anwender, R.; Runte, O.; Eppinger, J.; Gerstberger, G.; Herdtweck, E.; Spiegler, M. Synthesis and Structural Characterization of Rare-Earth Bis(dimethylsilyl)amides and Their Surface Organometallic Chemistry on Mesoporous MCM-41. *J. Chem. Soc., Dalton Trans.* **1998**, 847–858.

(31) Yuen, H. F.; Marks, T. J. Phenylene-Bridged Binuclear Organolanthanide Complexes as Catalysts for Intramolecular and Intermolecular Hydroamination. *Organometallics* **2009**, *28*, 2423–2440.

(32) Eppinger, J.; Spiegler, M.; Hieringer, W.; Herrmann, W. A.; Anwender, R. C₂-Symmetric ansa-Lanthanidocene Complexes. Synthesis via Silylamine Elimination and β -SiH Agostic Rigidity. *J. Am. Chem. Soc.* **2000**, *122*, 3080–3096.

(33) Parkin, G., Classification of Organotransition Metal Compounds. In *Comprehensive Organometallic Chemistry III*; Mingos, D. M. P., Crabtree, R. H., Eds.; Elsevier: 2007; pp 1–57.

(34) Green, M. L. H. A New Approach to the Formal Classification of Covalent Compounds of the Elements. *J. Organomet. Chem.* **1995**, *500*, 127–148.

(35) Rees, W. S.; Just, O.; Schumann, H.; Weimann, R. Structural Characterization of a Tris-Agostic Lanthanoid-H-Si Interaction. *Angew. Chem., Int. Ed. Engl.* **1996**, *35*, 419–422.

(36) Eedugurala, N.; Wang, Z.; Yan, K.; Boteju, K. C.; Chaudhary, U.; Kobayashi, T.; Ellern, A.; Slowing, I. I.; Pruski, M.; Sadow, A. D. β -SiH-Containing Tris(silazido) Rare-Earth Complexes as Homoge-

neous and Grafted Single-Site Catalyst Precursors for Hydroamination. *Organometallics* **2017**, *36*, 1142–1153.

(37) Brookhart, M.; Green, M. L. H.; Wong, L. L. Carbon Hydrogen Transition-Metal Bonds. *Prog. Inorg. Chem.* **1988**, *36*, 1–124.

(38) Clot, E.; Eisenstein, O., Agostic Interactions from a Computational Perspective: One Name, Many Interpretations. In *Principles and Applications of Density Functional Theory in Inorganic Chemistry II*; Kaltsoyannis, N., McGrady, J. E., Eds.; Springer Berlin Heidelberg: 2004; Vol. 113, pp 1–36.

(39) Procopio, L. J.; Carroll, P. J.; Berry, D. H. Agostic Beta-Si-H Interactions in Silylamido Complexes of Zirconocene. *J. Am. Chem. Soc.* **1994**, *116*, 177–185.

(40) Yan, K.; Duchimaza Heredia, J. J.; Ellern, A.; Gordon, M. S.; Sadow, A. D. Lewis Base Mediated β -Elimination and Lewis Acid Mediated Insertion Reactions of Disilazido Zirconium Compounds. *J. Am. Chem. Soc.* **2013**, *135*, 15225–15237.

(41) Yan, K.; Pindwal, A.; Ellern, A.; Sadow, A. D. Direct Hydrosilylation by a Zirconacycle with β -Hydrogen. *Dalton Trans.* **2014**, *43*, 8644–8653.

(42) Boteju, K. C.; Wan, S.; Venkatesh, A.; Ellern, A.; Rossini, A. J.; Sadow, A. D. Rare Earth Arylsilazido Compounds with Inequivalent Secondary Interactions. *Chem. Commun.* **2018**, *54*, 7318–7321.

(43) Shinohara, K.; Tsurugi, H.; Anwender, R.; Mashima, K. Trivalent Rare-Earth Metal Amide Complexes as Catalysts for the Hydrosilylation of Benzophenone Derivatives with $\text{HN}(\text{SiHMe}_2)_2$ by Amine-Exchange Reaction. *Chem. - Eur. J.* **2020**, *26*, 14130–14136.

(44) Lin, C.-Y.; Guo, J.-D.; Fettinger, J. C.; Nagase, S.; Grandjean, F.; Long, G. J.; Chilton, N. F.; Power, P. P. Dispersion Force Stabilized Two-Coordinate Transition Metal–Amido Complexes of the $-\text{N}(\text{SiMe}_3)\text{Dipp}$ ($\text{Dipp} = \text{C}_6\text{H}_5-2,6\text{-iPr}_2$) Ligand: Structural, Spectroscopic, Magnetic, and Computational Studies. *Inorg. Chem.* **2013**, *52*, 13584–13593.

(45) Lin, C.-Y.; Fettinger, J. C.; Grandjean, F.; Long, G. J.; Power, P. P. Synthesis, Structure, and Magnetic and Electrochemical Properties of Quasi-Linear and Linear Iron(I), Cobalt(I), and Nickel(I) Amido Complexes. *Inorg. Chem.* **2014**, *53*, 9400–9406.

(46) Schadle, C.; Meermann, C.; Tornroos, K. W.; Anwender, R. Rare-Earth Metal Phenyl(trimethylsilyl)amide Complexes. *Eur. J. Inorg. Chem.* **2010**, *2010*, 2841–2852.

(47) Schumann, H.; Winterfeld, J.; Rosenthal, E. C. E.; Hemling, H.; Esser, L. Organometallic Compounds of the Lanthanides. 88. Monomeric Lanthanide(III) Amides: Synthesis and X-ray Crystal Structure of $[\text{Nd}\{\text{N}(\text{C}_6\text{H}_5)(\text{SiMe}_3)_2\}_3(\text{THF})]$, $[\text{Li}(\text{THF})_2(\mu\text{-Cl})_2\text{Nd}\{\text{N}(\text{C}_6\text{H}_5\text{Me}_2-2,6)(\text{SiMe}_3)_2(\text{THF})\}_2]$, and $[\text{ClNd}\{\text{N}(\text{C}_6\text{H}_5\text{-iso-Pr}_2-2,6)(\text{SiMe}_3)_2(\text{THF})\}_2]$. *Z. Anorg. Allg. Chem.* **1995**, *621*, 122–130.

(48) Wang, S.-w.; Qian, H.-m.; Yao, W.; Zhang, L.-j.; Zhou, S.-l.; Yang, G.-s.; Zhu, X.-c.; Fan, J.-x.; Liu, Y.-y.; Chen, G.-d.; Song, H.-b. Synthesis of Rare Earth Metal Complexes Incorporating Amido and Enolate Mixed Ligands: Characterization and Reactivity. *Polyhedron* **2008**, *27*, 2757–2764.

(49) Deacon, G. B.; Forsyth, C. M.; Scott, N. M. Solvent-Free Lanthanoid Complexes Derived From Chelation-Supported Organamide Ligands. *Eur. J. Inorg. Chem.* **2002**, 1425–1438.

(50) Chao, Y. W.; Wexler, P. A.; Wigley, D. E. Preparation and Properties of Tantalum Imido Complexes and Their Reactions with Alkynes. Coordination Control Through Multiple Metal-ligand Bonding. *Inorg. Chem.* **1989**, *28*, 3860–3868.

(51) Wiseman, G. H.; Wheeler, D. R.; Seyferth, D. Preparation of Cyclodisilazanes From Dimethylhydroaminosilanes, $(\text{CH}_3)_2\text{Si}(\text{H})\text{-NHR}$. *Organometallics* **1986**, *5*, 146–152.

(52) Perrin, C. L.; Dwyer, T. J. Application of Two-dimensional NMR to Kinetics of Chemical Exchange. *Chem. Rev.* **1990**, *90*, 935–967.

(53) Parks, D. J.; Piers, W. E. Tris(pentafluorophenyl)boron-catalyzed Hydrosilylation of Aromatic Aldehydes, Ketones, and Esters. *J. Am. Chem. Soc.* **1996**, *118*, 9440–9441.

(54) Herrmann, W. A. *Synthetic methods of organometallic and inorganic chemistry*; Thieme Medical: 1996; Vol. 6.